Utrecht University

Veterinary Medicine

Major internship report

Setting up a cellular assay to characterize regulation of functional docking of the proteasomal activator PA28αβ within the antigen processing pathway

PA28 phosphorylation as a possible regulatory mechanism

Holtrop, A.F. (Anne Floor)

2020-2021

Table of content

Author: Anne Floor Holtrop
Student number: 2692554
Master Program: Molecular and Cellular Life Sciences
Major Research Project: Report
Duration internship: 30 November 2020 – 17 November 2021
Department: Biomolecular Health Sciences, Infectious diseases and immunology, Alice Sijts group, University Utrecht

Daily supervisor: M. Wawrzyniuk
Primary examiner: Dr E. J. A. M. Sijts
Secondary examiner: Dr B. Kleizen

Date: 21th of November 2021

0. Layman's summary.

To ensure that all the cells in your body are working properly, it is important that unnecessary and damaged proteins are cut into inactive fragments by the disposal system. In diabetes and some cancers, not all proteins are cleared properly by this system. Often this is the result of a poorly functioning protein complex, called the proteasome. The proteasome is a barrel-shaped protein complex that normally functions as a so-called "protein-scissor". Fragments cut by the proteasome can be recycled or be positioned as a flag on the outside of the cell. This flag shows patrolling cells in the body what that cell is working on. If the flag shows that that cell is either not working properly or that it is sick, these patrolling cells make sure that cell gets cleaned up. Since you do not want useful proteins to be cut, the proteasome is usually inactive. To activate the protein-scissor, the scissor needs to be opening up the barrel. The pressure needed for this is given by a "cap". One such cap is PA28, which is a protein complex consisting of 2 different units: named PA28α and PA28β. If PA28 is working in the cell, it can influence the flag types that are positioned on the outside of the cell.

The binding between the proteasome and PA28 involves two parts: 1) physical contact between the two units and 2) activation of the protein-scissor. From previous research, we know that PA28α is crucial for initiating physical contact, especially with its last building block. Moreover, without a charge somewhere in PA28α, the binding does not work, but if this charge impairs physical contact or activation of the protein-scissor remains unclear. To look into this idea, this study started with adding a tag to PA28α to be able to gather every PA28 complex in the cell to see if it is bound to the proteasome. Furthermore, this study aimed to improve a method to collect all PA28 within the cell by pulling it out. Second, since interacting with the proteasome is not the only process involved in opening the barrel, this study also aimed to improve the way to look at the functionality of the activation of the proteasome by looking at certain flag types. Especially if different charges are applied to the last building block of PA28α.

This study was the first step in creating a model to look at the functional interaction between PA28 and the proteasome. Several questions arose during the improvement of the experiments which warrant further investigation. If we would ever be able to improve the functionality of the protein-scissor by targeting its interaction with PA28, we might be able to treat people suffering from diabetes and the cancers which are related to abnormal levels of PA28.

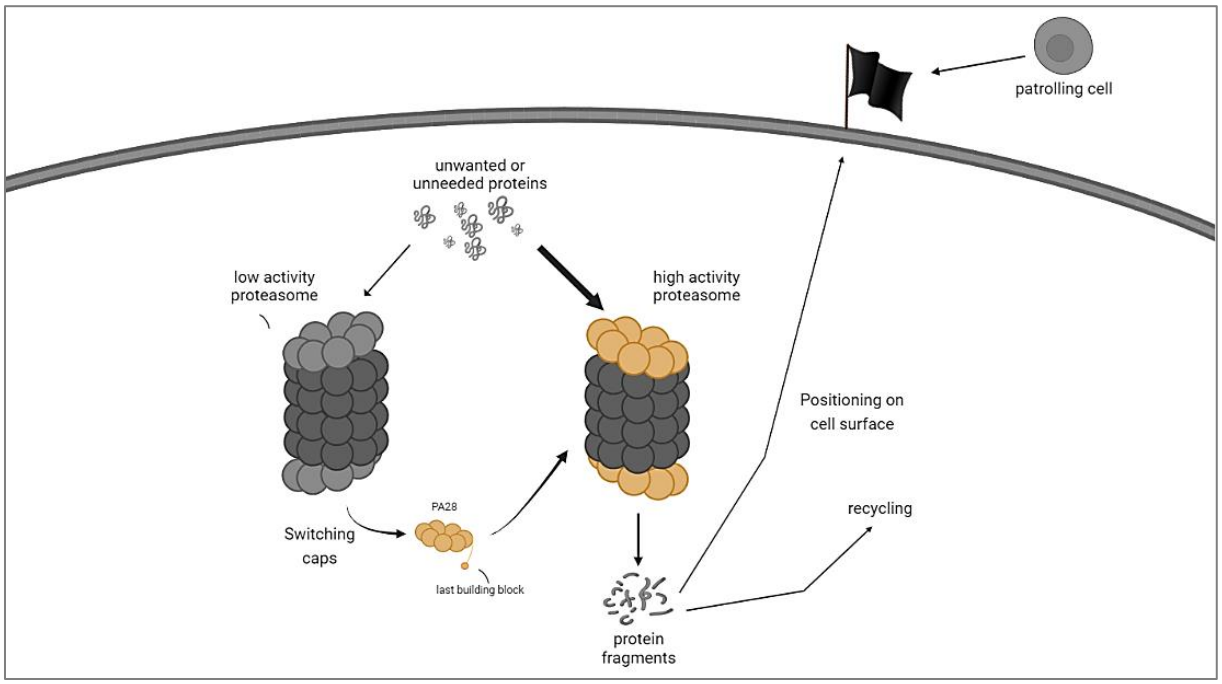

Graphical abstract Layman's summary.

Setting up a cellular assay to characterize regulation of functional docking of the proteasomal activator PA28αβ within the antigen processing pathway

Holtrop, A.F.

The proteasome activator 28 (PA28αβ) regulates both the influx of substrates through the terminal rings of the proteolytic core, and the proteolytic activity of the core particle (CP). Functional docking of PA28αβ onto the CP involves 1) the physical interaction between the two complexes, and 2) the activation of the proteolytic activity of the CP. Physical docking requires the insertion of the last carboxyl-terminal tyrosine of PA28α into the outer rings of the CP. Another factor involved in docking is a phosphorylated amino acid in PA28αβ, as the dephosphorylation of this complex abolishes stimulating abilities. As phosphorylation patterns of PA28αβ change within the cell due to stimulation, the question arose if this change is used as a regulatory mechanism for docking of it onto the CP. Therefore, this study aimed to set up a cellular assay to characterize the docking behaviour of PA28αβ in murine Ana-1 macrophages. Experiments were performed using stable, monoclonal cell lines of WT, and PA28β-deficient murine macrophages, obtained by utilizing the CRISPR/Cas9 gene editing system, and were performed in both unstimulated and interferon-gamma stimulated cells. First, expression of both PA28αβ subunits was determined via quantitative western blot and flow cytometry analysis. Secondly, Ana-1 cells were treated with the CRISPR/Cas9 gene editing system. In the first way, in both wildtype and ΔPA28β Ana-1 macrophages an affinity tag was inserted at the N-terminus of the Psme1 gene, encoding for PA28α, and this was validated using flow cytometry analysis. The second way, via utilizing error-prone DNA repair, the efficiency and efficacy of single guide RNAs (sgRNAs) was investigated. Subsequently, genotyping was performed to validate if the designed single guide RNAs (sgRNAs) targeted the Cas9 enzyme to the right cutting site in Cas9-treated Ana-1 macrophages. Lastly, a immunoprecipitation protocol was partly optimised with the intention to isolate PA28αβ out of the cell to study its docking behaviour. I found that PA28β is upregulated in response to stimulation, whereas PA28α levels remain unaffected. However, the question arose how successful stimulation of the cells had been, as the major histocompatibility complex class I levels remained unaffected too. The insertion of the affinity tag was successful, but any result was abolished after a freeze-and-thaw-cycle. Lastly, immunoprecipitation remained unsuccessful, and still needs several optimisation steps. Unravelling the highly complex interconnection of pathways influencing proteins' fate from synthesis to degradation is fundamental to improve our understanding of the interplay between cellular proteostasis and the immune system before we are able to specifically target it during therapy.

Keywords: *PA28 • Antigen Processing • Functional docking • IFN-γ • Phosphorylation • Optimisation*

1. Introduction.

The term “proteasome” refers to a highly conserved set of proteins that play a central role in the degradation of damaged, unnecessary, and misfolded proteins within the cell. Removal of proteins by the proteasome is either used for stagnation of (signalling) pathways or to prevent accumulation and deleterious effects. Therefore, the proteasome is crucial in a variety of cellular pathways,[1,2] including cell-cycle progression, signal transduction, protein quality control and antigen presentation.[3,4]

A constitutive proteasome embodies a 20S multicatalytic, barrel-shaped core (a.k.a. core particle, CP), formed by the axial stacking of four heptameric rings (**Fig. 1a**),[5] which comprises two outer α-rings and two inner β-rings in an αββα fashion.[5–7] The three enzymatic residues (termed β1, β2 and β5) reside in the internal β-ring cavity of the CP (**Fig. 1b**).[8] After interferon-γ (IFN-γ) stimulation, newly synthesised proteasomes incorporate the so-called immuno-counterparts of these catalytic sites (β1i, β2i and β5i, respectively), forming the immuno-proteasome.[9] The changed enzymatic properties of the immunoproteasome, compared to the constitutive proteasome, favours the production of major

Abbreviations used: *CP, core particle; IFN-γ, interferon-γ; MHC, major histocompatibility complex; RP, regulatory particles; PA28, proteasome activator 28; CRISPR, clustered regularly interspaced short palindromic repeats ; CRISPR-associated protein 9, Cas9; homology directed repair, HDR; Y, tyrosine; K, lysine; IP, immunoprecipitation; WT, wildtype; KI, knock-in; KO, knock-out; FBS, heat inactivated fetal bovine serum; P/S, penicillin/streptomycin; β-ME, β-mercapto-ethanol; sgRNA, single guide RNA; bp, base pair; MQ, milliQ; NHEJ, nonhomologous end-joining; Ab, antibody; PVDF, polyvinylidene fluoride;*

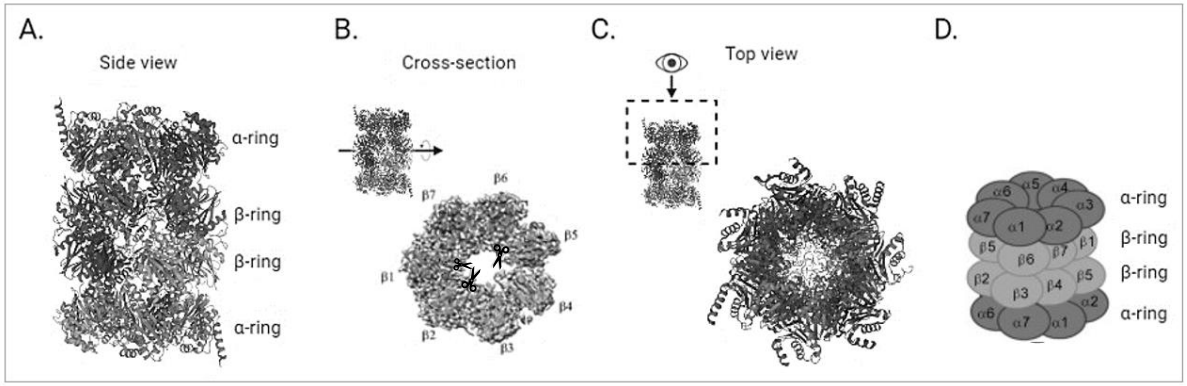

Figure 1: Cryo-electron microscopy and schematic structure of the human 20S core particle*. The cryo-EM structures of* ***a)*** *the 20S core particle (CP, PBD: 6RGQ),* ***b)*** *a cross-section of the β-catalytic chamber, [90] and* ***c)*** *its enlarged top view. Catalytic sites are depicted as scissors.* ***d)*** *A schematic representation of the core, originates from Pickering and Davies (2012).[92] The cryo-EM structures were adapted from literature.[32,93]*

histocompatibility complex (MHC) class I binding peptides and is therefore involved in the antigen presentation pathway.

As the NH_2-terminal termini of the outer α-rings occlude the access to the catalytic sites (**Fig. 1c**),[6,10,11] unwanted proteolysis of cytosolic proteins is mainly prevented.[12] Accordingly, the opening of this so-called α-gate, and thereby allowing access for substrates into the catalytic chamber,[13] is tightly regulated through the association of the proteasome with regulatory particles (RPs), including the 19S (a.k.a. PA700), the PA200, and the 11S regulators PA28αβ and PA28γ.[2,14]

The proteasome activator 28 αβ (PA28αβ) (~180 kDa) is an IFN-γ induced complex that can associate with either ends of the 20S core particle.[15,16] In mammals, PA28αβ is composed of two nonidentical but homologous subunits (hereafter, termed PA28α and PA28β),[17] that form an oligomeric structure within the cell (**Fig. 2**).[18] The stoichiometry of the oligomer remains a matter of debate, with some studies claiming it forms a heterohexameric structure of $(αβ)_3$,[19] whereas other studies report heteroheptameric variants that have an alternating α- and β-subunit arrangement with either a single α-α,[20] or a β-β interface.[21,22]

The exact molecular mechanism of how PA28αβ alters the cleavage behaviour of the CP remains elusive. To date, it is known that there is a change in the average length of peptides leaving the proteasomal core,[23,24] and that this change is associated with enhanced generation of MHC class I antigenic peptides.[25–28] This may result from the enhanced double-cleavage activity and decreased single-cleavages,[24] and the fact that PA28αβ retains longer protein substrates in the β-cavity until the fragments are small enough to diffuse into the cytosol.[23] Taking this together with the fact that both PA28α and PA28β are upregulated due to stimulation with the major immunomodulatory cytokine IFN-γ, emphasizes the fact that at least one of the *in vivo* functions of PA28αβ resides within the immune recognition of (viral) infected and malignant host cells. Nevertheless, it is important to note that the association of either one or two PA28αβ complexes with the 20S proteasome does not result in enhanced or changed rates of protein degradation,[23,29] but only noticeably modifies the pattern produced.[23]

Biochemical data substantiates the notion that functional docking (i.e. binding with and activation of its target) of PA28αβ onto the proteasome encompasses two different mechanisms.[30,31] Initially,

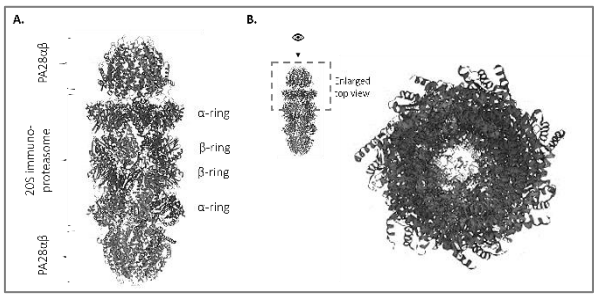

Figure 2: Cryo-electron microscopy structure of two PA28αβ caps docked on either site of the 20S immunoproteasome. *In* ***a****. and* ***b.,*** *a cryo-EM structure is shown of* ***a.*** *PA28αβ docked onto the immune-proteasome (PBD: 7DRW) and* ***b.*** *an enlarged top view of the same structure.*

during docking, the last five carboxyl-terminal amino acids of at least four subunits of PA28αβ are inserted into the α-ring pockets of the 20S particle.[32] Out of these five, presence of the last tyrosine in the PA28α subunits is vital, since deletion of or conversion to charged amino acids in isolated proteins results in complexes unable to both stimulate the peptidase activity of the CP,[6,33,34] and to dock on it.[6,33] The interaction between the carboxyl-terminal termini and The 20S proteasome most likely results in a conformational change in the α-rings of the proteasome in which the N-terminal sequences blocking the cavity entrance are pulled up.[35] These rearrangements result in an unobstructed path into the β-chamber.[35] Subsequently, an activation loop and a neighbouring proline residue on one face of PA28α subunits and a virtually identical sequence in PA28β presumably provide the required energy for the activation of the hydrolytic capacities of the proteasome.[30]

Besides the presence of the activation loop and the last carboxyl-terminal tyrosine of PA28α, also phosphorylation of PA28αβ is believed to play a role in the process of functional docking. The fact that (de)phosphorylation within the proteasomal system can be used as a regulatory mechanism has already been established. For example, IFN-γ treatment decreases phosphorylation levels on several subunits in the CP, resulting in destabilised 26S proteasome and an increase of PA28αβ-containing complexes.[36] Moreover, dephosphorylation of PA28αβ abolishes any stimulating activity of the proteasome.[34] However, which specific residues of PA28α are phosphorylated, and how the phosphorylation status can change within a cellular context has not been studied in detail yet.

This study took the first step in answering the question whether the phosphorylation status of the last carboxyl-terminal tyrosine residue of PA28α (hereafter termed 249Y) influences the docking propensity of PA28α on the 20S proteolytic core in murine macrophages. First, the clustered regularly interspaced short palindromic repeats (CRISPR)/CRISPR-associated protein 9 (Cas9) system, together with homology-directed repair (HDR) templates designed in a preceded study,[37] were used for inserting a FLAG-tag in front of the endogenous gene encoding for PA28α: *Psme1*. Subsequently, the same method was used to optimise this system to replace the 249Y amino acid for either phenylalanine or glutamic acid and to replace the 239K amino acid for a stop codon to remove the last disordered segment of the protein. Second, the protocol for a immunoprecipitation (IP) was partly optimised to extract PA28β from cell-lysates, which in turn was analysed by western blots for the presence of PA28β.

Until now, a variety of pathologies have already been linked to either overexpressing,[38–42] or downregulation of the PA28α subunit specifically.[43] Therefore, changed levels of it can potentially be utilised as a biomarker to either predict the prognosis,[44] assessment of, [43] or relapse probability of several diseases.[45] Underscoring the demand for an improved understanding of the underlying molecular pathways PA28αβ functions in, and to find the mechanism behind docking of this regulatory particle onto the CP before we can target it specifically in therapy.

2. Material & Methods.

2.1 Cell cultures.

All wildtype (WT), knock-in (KI) and knock-out (KO) Ana-1 macrophages (derived from C57Bl/6 (B6, H-2K^b) mice) were cultured in RPMI-1640 + GlutaMAX^{TM} (Gibco, USA) medium supplemented with 10% heat inactivated fetal bovine serum (FBS) (Bodinco BV; Netherlands), 1% penicillin/streptomycin (P/S) (Gibco; USA), and 0,1% β-mercapto-ethanol (β-ME) (Millipore Corporation, USA), hereafter termed "full medium". Cells were maintained at 37^{o}C in a fully humidified incubator with an atmosphere of 5% CO_2.

2.2 Functional concatemer targeting 249Y and 239K.

2.2.1 sgRNA design.

For designing single guide RNAs (sgRNAs), targeting murine *Psme1* (Gene ID: 19186; imported sequence: NBIM37, mm9, *Mus musculus*), the CRISPR tool to "design and analyse guides" (default settings) of the Molecular Biology CRISPR design tool Benchling (*https://benchling.com/*, version 2020_12) database was utilized.

The first sgRNA was designed as to modify the last carboxyl-terminal tyrosine of PA28α, referred to as 249Y, to assess the effect of different phosphorylation statuses on docking propensity. A total of 7 possible sgRNAs were proposed by Benchling to cut within a range of 20bp of this target (**Tab. S1**). Considering their on- and off-score values, 4 out of 7 had an on-score >40

Table 1: Potential sgRNAs selected from Benchling using the Psme1 gene as input query. *Data copied from Benchling. Abbreviations: PAM, protospacer adjacent motif.*

Target	Cutting position	Sequence of the sgRNAs	PAM type	On-target score	Off-target score
249Y	56200227	CCCATCACAGAATGAGAGAG	GGG	66.8	26.5
239K	56200199	GAAGCCCCGTGGAGAAACCA	AGG	30.1	28.1

Table 2: Off-target score clarification of possible sgRNA targeting 249Y and 239K. *Data copied from Benchling. Only showed scores of 1.5 or higher. Highlighted in bold: variation of the sequence of the sgRNA which the Cas9 enzyme could recognise too. Abbreviations used: PAM, protospacer adjacent motif; Chr, chromosome.*

Target	Sequence	PAM	Score	Gene	Locus
249Y	CCCATCACAGAATGAGAGAG	GGG	100,0	Psme1 (ENSMUSG00000022216)	Chr14:-55581390
	CCCATCACAGAACGAGAGAG	GGG	38,7	/	Chr1:+91171422
	ACCATCACAGAATGAGAGAA	GGG	10,4	/	Chr15:-5464923
239K	GAAGCCCCGTGGAGAAACCA	AGG	100.0	RP24-148E21.3 (ENSMUSG00000100018)	Chr1:-91171449
	GAAGCCCCGTGGAGAAACCA	AGG	100.0	Psme1 (ENSMUSG00000022216)	Chr14:+55581362
	CTA**A**CCC**A**GTGGAGAAACCA	TGG	1.5		Chr9:+115664390

but neither had an off-score >60. After examination of the off-target values, it was found that the low off-target value of one of the options with the highest on-score (**Tab. 1**) was mainly due to a non-coding region on chromosome 1, according to Benchling, (**Tab. 2**).

To reconfirm that the carboxyl-terminal disordered segment of PA28α is involved with docking, a sgRNA was designed to remove this part by introducing a stop codon at the start of this segment. Using the UniProt database (*https://www.uniprot.org/*, version 2020_12) provided sequence of PA28α, it was determined that there is a disordered segment, starting from the 239th amino acid, it being a lysine (K), hereafter termed 239K. Again, using the CRISPR tool of Benchling, two options were proposed (**Tab. S2**) targeting 239K, of which none were considered optimal due to low on- and off-values. Again, after assessing the reason behind the low values, it was found that the low-off score was predominantly due to the presence of a pseudogene (RP24-148E21.3, gene ID (MGI): 665577) on chromosome 1. The sgRNA with the cutting site closest to the target site was chosen.

Lastly, to ensure insertion of the sgRNAs into the cassettes of the concatemer (paragraph 2.2.3), overhangs were added (**Tab. S3**). All sequences were ordered from ThermoFisher (USA) as primers.

2.2.2 Homology directed repair (HDR) design.

To modify the 249Y of *Psme1* at the carboxyl-terminus, without creating unwanted mutations, a single stranded DNA sequence complementary to the target DNA needs to be provided to induce HDR repair instead of error-prone nonhomologous end-joining (NHEJ). An HDR template contains intended mutations or insertions which are flanked by homologous regions to the target DNA. Templates in this study are linear, single-stranded DNA strands.

Herefore, the same steps were performed as described in a previous study for inserting the FLAG-tag (a.k.a. DYKDDDDK-tag or affinity tag) at the N-terminal site of *Psme1.*[37] The design and ordering of the template was performed by M. Wawrzyniuk.

Briefly, using the default settings [genome of GRCm38 (mm10, Mus musculus) and an NGG (SpCas9 3'side) PAM sequence], the amino acid was changed to the most frequent codon used by the Mus Musculus for either amino acid F (TTC; freq = 21,8) or E (GAG; freq = 39,4). The upstream arm was set on 114 bp and the downstream arm on 121 bp. Next, the guide designed for targeting either 249Y or 239K (**Tab. 1**) was inserted to create a template that prevents recutting. Afterwards, they were ordered at ThermoFisher (USA) as primers to anneal later on into guide RNAs (gRNAs). The complete HDR sequences can be found in the supplementary data (**Tab. S4**).

2.2.3 Generation of gRNA plasmids.

All primer pairs of paragraph 2.2.1 were cloned into an murine stem cell virus retroviral plasmid containing two repetitive gRNA expression cassettes (**Fig. S1**), kindly provided by Dr. A. Merenda, using a protocol for multiple gene knockouts with minor changes.[46]

Briefly, 5' ends of gRNA oligos (10 mM mix of forward and reverse primers were phosphorylated and annealed in a BioRad thermocycler (Bio-Rad Laboratories B.V., USA), together with 2 µL T4 DNA ligase buffer (10x), 3 µL gRNA top strand (10 µM), 3 µL

gRNA bottom strand (10 µM), 1.0 µL T4 PNK (all ordered from New England Biolabs; UK) and H2O added up to a total volume of 20.0 µL. The settings were as followed: 37°C for 30 min, 95°C, ramp down to 25 °C at 0,5 °C/min and hold at 4°C. Subsequently, a *Bbs*I shuffling reaction was performed by ligating the annealed gRNAs in the concatemer using 0,4 µL CRISPR-concatemer vector (kind gift from A. Merenda), BSA-containing restriction enzyme buffer (10x), 1,0 µL DTT (10 mM), 1,0 µL ATP (10 nM), 1,0 µL *Bbs*I, 1,0 µL T7 ligase (all ordered from New England Biolabs; UK) and 4,6 µL Milli-Q (MQ). Again, the thermocycler was used and used at the following settings: 35 cycles at 37 °C for 5 min, 21 °C for 5 min, held at 37 °C for 15 minutes, then it was hold at 4°C.

Next, exonuclease treatment was performed to increase the efficiency of the cloning procedure. First, after thawing *E. coli* TOP10 cells (ThermoFisher; USA) from the freezer (-80°C), the plasmids (i.e. concatemer with cassettes possibly filled with annealed gRNAs) were added to the cells and incubated for 20 minutes on ice. A heat shock was subsequently applied using a heat-block set at 42°C for 90 seconds, followed by 60 seconds on ice. Next, 400 µL S.O.C.-medium (Invitrogen; USA) was added, and the cells were incubated for 50 minutes at 37°C while shaking. Subsequently, the bacteria were plated on agar plates supplemented with ampicillin (Biotrading; Netherlands) and grown overnight at 37°C. The corresponding transformants were grown at 37°C in liquid broth medium (Biotrading; Netherlands) supplemented with 1% ampicillin sodium salt (Sigma-Aldrich; China.

The day after, the bacteria were collected, and a Zyppy™ Plasmid Miniprep Kit (Lot No.: ZRC201215; Zymo Research; USA) was used to extract plasmids according to the manufacturer's instructions. Next, vector sequencing was performed by adding ~200 ng of DNA, 2.5 µL 10 mM of Forward Primer (either TCAAGCCCTTTGTACACCCTAAG for cassette 1 or GACTACAAGGACGACGATGACAA for cassette 2; both ordered at ThermoFisher; USA), and MQ up to 20 µL in a tagged Eppendorf and submitted for sequencing by Macrogen (Netherlands).

The program Chromas version 2.6.5 was used to analyse the sequencing results. If at least one of the two cassettes was filled with gRNA targeting either 249Y or 239K, a Quantum Prep Plasmid Midiprep Kit (Bio-Rad; USA) was performed, using the provided instructions, to amplify the number of plasmids and used for the generation of the different cell lines.

2.3 Electroporation.

On the day prior to electroporation, the medium of the Ana-1 cells (60-80% confluency) was changed to RPMI-1640 medium, supplemented with 5% heat-inactivated FBS, 1% Penicillin/Streptomycin and 0,1% β-ME.

On the day of electroporation, 1 almost full grown 10 cm dish (cells in log phase) per condition were collected and resuspended in 200 µL warm RPMI-1640 medium (37°C) and subsequently transferred to 0.4 mm electroporation cuvette caps (Bio-Rad Laboratories B.V. ; USA). Afterwards, the Cas9 encoding plasmid (688 ng/µL), and both the HDR template (750 ng) and the gRNA designed and ordered by L.G. Masselink,[37] were added to the cuvette to insert the FLAG-tag N-terminally of *Psme1*, with a ratio of 4:1:12 in terms of ng, respectively. As a control for functionality of this method, 3, 6 and 9 µL of eGFP plasmid only was used for electroporation.

Electroporation was performed in a GenePulser (Bio-Rad Laboratories B.V. ; USA), using the following setting: voltage 250V, high capacitance of 975 uF and resistance being infinite. After 5-10 min, the content of the cuvette was plated onto a 6 cm treated dish (Corning BV; Netherlands). Cells which were treated with the CRISPR/Cas9 system components (i.e. cas9- and sgRNA- (115.1 and 246.6 ng/µL for targeting 239K and 249Y, respectively) containing plasmids, and corresponding HDR template) to check the functionality of the sgRNAS were electroporated following the same protocol as described above. ~24h after electroporation, the medium was changed to full medium supplemented with 7.5 ng/mL puromycin (Merck; Germany) for ~48, to select for cells which internalised and subsequently expressed the gRNA containing concatemer. After the ~48h, the cells were cultured in full medium and upscaled until further use. If the eGFP encoding-plasmid was electroporated, no selection procedure was performed. For these cells, after 24-30h expression of eGFP was visualized with light microscopy.

2.4 Genotyping.

2.4.1 Primer design for genotyping.

Primers targeting the disordered C-termini of PA28α (Accession number: AB007136, version AB007136.2) were designed using the program Primer-

Table 3: picked primers for amplifying (part) of exon 11 of Psme1. Primer pairs designed using the NCBI nblast tool and ordered at ThermoFisher (USA). Primer pairs that showed up during the design but weren't chose are not shown. *Abbreviation used: Tm, melting temperature.*

Primer pair	Sequence (5'->3)	Length	Start	Stop	Tm	Product length
2	*Forward*: CTCTGTGCTCCGATAGGCTG	20	4413	4432	59.97	338
	Reverse: AACCAGCGGCTTAACACTCA	20	4750	4731	59.89	
7	*Forward*: CAAGACGCGTTCTTTGCTCC	20	4735	4754	60.11	1053
	Reverse: CCAACCAGCGGCTTAACAC	19	4906	4887	59.42	
10	*Forward*: TCACTGCCTTGGAAAGGGTG	20	2840	2859	60.18	1909
	Reverse: CCAGCGGCTTAACACTCAAATC	22	4748	4827	60.16	

Blast of the National Centre for Biotechnology Information (NCBI, *http://www.ncbi.nlm.nih.gov,* version 2021_02). Default settings were used with a minor change: the PCR product size was increased to 3000. Out of the 10 primer pairs arising, 9 would amplify the last part of exon 11 (data not shown). Three pairs were picked randomly (**Tab. 3**), one comprising whole exon 11, one which would amplify only the last part of exon 11, and one with an in-between length compared to the previous mentioned primers. The primers were ordered at ThermoFisher (USA).

2.4.2 Genomic extraction.

A Purelink genomic DNA Mini Kit (Ref.: K1820-02; Lot No.: 1690730; Invitrogen; USA) was used to extract the DNA out of the Ana-1 cells, according to the manufacturer's instructions.

To confirm genomic extraction succeeded, a digestion reaction was performed using either 50, 200 or 500 ng of plasmid (according to the absorbance at 280 nm, using nanodrop-1000 v.3.8.1), 1.0 µL of NRU1 enzyme (Life Technologies; USA) and 2 µL CutSmart buffer (New England Biolabs; UK), topped up to 20 µL with MQ. The samples were left in room temperature for ~90 min. Subsequently a 1% agarose gel (1% Ultrapure™ Agarose (Invitrogen; USA) in 0.5 TBE Electrophoresis Buffer (Thermo Fisher Scientific Baltics; Lithuania), supplemented with 2.5 µL Midori Green (NIPPON Genetics EUROPE; Germany), was run at 90V.

2.4.3 PCR reaction.

To amplify the part of the genome of interest, a PCR reaction was performed. For the reaction itself, a mix of 0,2 µL GoTaq G2 Flexi DNA polymerase, 2 µL dNTPs, 2,4 µL $MgCL_2$, 8 µL 5x Green GoTaq Flexi Buffer (all ordered at Promega; USA), 50-100 ng DNA, and 4 µL of 5' ends of primer pairs (10 mM mix of corresponding forward and reverse primers) topped up to 40 µL with MQ was used. As a positive control, a forward and reverse primer pair and a plasmid (expected height ~8000 kDa) was kindly provided by F. Pashaie. The settings for the PCR reaction in a thermocycler were as followed: 95°C for 5 min, 28 cycles with 15 seconds at 95°C, 62.2 °C for 15 seconds and 72 °C for 30 sec, followed by 5 min at 72 °C, then held at 12°C until pickup.

For determination of which primer pair to proceed with, another PCR reaction was performed, using a mix of 10 µL 5x polymerase buffer, 2,5 µL DSMO, 2,5 µL dNTPs, 0,35 µL of the Q5 enzyme (all ordered at New England Biolabs; UK), ~200 ng genomic DNA, 5 µL of 5' ends of primer pairs (10 mM mix of corresponding forward and reverse primers, **Tab. 3**) and topped up to 50 µL with MQ. For this, a BioRad thermocycler was used with the following settings: 95°C for 3 min, 34 cycles with 30 seconds at 95°C, 56 °C for 30 seconds and 72 °C for 2 min, followed by 5 min at 72 °C, then 12°C forever.

2.4.4 Gel electrophoresis and purification.

To separate the PCR product from potential background or aspecific products, 15 µL of the PCR product and 5 µL of the 50bp ladder (ThermoFisher; Netherlands) was resolved onto a 1% agarose gel. The gel was supplemented with 2.5 µL Midori Green (NIPPON Genetics EUROPE; Germany) and run at 90V for 45-70 min. Presence of bands was determined with a Geldoc Transilluminator (Bio-Rad Laboratories; USA) and bands with the expected height (~350-400 kDa) were cut out with a sharp razor. Last, a Zymoclean™ Gel DNA Recovery Kit (Cat. No.: D4001; Lot No.: ZRC187655; Zymo research; USA) was used to extract the DNA out of the gel according to the manufacturer's instructions.

2.4.5 Sanger sequencing.

200 ng extracted DNA out of the agarose gel, 10 mM of a Forward Primer (**Tab. 3**), and MQ up to 20 µL were added to a tagged Eppendorf and submitted

for sequencing by Macrogen (Netherlands). Analysis was not performed in this study.

2.5 Flow cytometry.

2.5.1 Extracellular staining.

The presence and the relative amount of MHC class I molecules was determined via flow cytometry. Briefly, ~0,5 million Ana-1 cells were fixated with CellFIX™ (1:10 dilution; Becton Dickinson; Belgium) for 30 min at room temperature. After washing twice with FACS buffer (2% FBS in PBS (Corning; USA)), the cells were stained with anti-mouse H-2K^b, FITC conjugated antibodies (Abs) (dilution 1:100; BD Biosciences; USA), for 30 min. Subsequently, the stained cells were washed twice with FACS buffer and resuspended in FACS buffer for measurement. Fluorescence was measured using a FACS Canto (BD Pharmingen, San Diego, CA, USA) flow cytometer with the FITC channel (495-519 nm).

The data was analysed using FlowJo version v10 Software. First the main population was selected in the programme (SSC vs FSC). Secondly the single cells were selected (FSC-A vs FSC-H). Lastly, non-stimulated cells were set as the "base level" of expression, meaning that the gates were placed in such a way that the majority cells from this set of cells were underneath it, to be able to compare it to stimulated cells.

2.5.2 Intracellular staining

For determining the effect of overnight IFN-γ stimulation on levels of PA28α and PA28β, an intracellular staining was performed. As described for an extracellular staining, Ana-1 cells, cultured overnight in the presence or absence of 12 mg/mL IFN-γ, were first washed twice with FACS buffer, and fixated with CellFIX for 30 min (RT). Subsequently, the cells were stained with the either the proteasome activator 11S α subunit (polyclonal antibody, cat no: BML-PW8185-0100; Enzo; USA) or proteasome activator 11S β subunit (polyclonal antibody, cat no: BML-PW8240; Enzo; USA) primary antibody. The antibodies were dissolved in FACS buffer supplemented with 0,2% saponin (Sigma; Netherlands), hereafter referred to as FACS-SAP, for 30 min. To wash away non-bound antibody, the cells were washed twice with FACS-SAP after which the DyLight 647 Donkey Anti-Rabbit IgG (minimal X-reactivity) (1:100 dilution; BioLedgend; USA) secondary antibody dissolved in the FACS-SAP, for 30 min. Finally, after washing twice with 50 µL FACS-SAP and once without saponin, the cells were resuspended in 180 µL FACS buffer

The intracellular staining for determining the presence of the FLAG-tag, follows the same workflow as described above, with the primary antibody being the M2 antibody anti-FLAG anti-mouse Ig (PE) (1:100 dilution; Sigma; Netherlands) antibody and the secondary antibody the PE labelled goat anti-mouse Ig (multiple adsorption) (1:100 dilution; A Becton Dickinson Co.; USA).

Fluorescence was measured using an HTS FACS Canto (BD Pharmingen, San Diego, CA, USA) flow cytometer. As described before, first the main population was selected and subsequently out of these cells the single cells were taken out for analysis. Lastly, looking at the negative control (WT cells stained with secondary Abs only), the threshold was determined (PE vs FSC) for cells which did not express the FLAG-tag. For analysis of PA28α and -β levels, the same gates were set, however, cells without stimulation overnight were set as the "base level" of expression.

2.6 Western blot.

Influence of IFN-γ stimulation on PA28α, PA28β was analysed by western blotting. Ana-1 cells were cultured overnight in the presence or absence of 12 mg/mL IFN-γ and subsequently harvested, washed, and lysed on ice with lysis buffer [50 mM Tris-HCL (Promega; USA), 150 mM NaCl (Merck; Germany), 5 mM EDTA (pH 8.0; Fluka; Germany), 1% NP-40 (Sigma; Netherlands), 0,05% NaN_3 (Merck; Germany); final pH of 7.4] for 30 min. Cell lysates were cleared by centrifugation (5 min, 14.000g, 4°C) and the extracted proteins in of the supernatant were denaturised by boiling the supernatant together with Laemmli buffer (Bio-Rad Laboratories; USA) for 10 min at 95°C.

The denaturised proteins and the Precision Plus Protein™ marker (Bio-Rad Laboratories; USA) were separated on a Mini-Protean® TGX™ Precast Gel (Bio-Rad Laboratories; USA) using 1x Tris/Glycine/SDS Buffer (Bio-Rad; USA) and transferred to a Immun-Blot® polyvinylidene fluoride (PVDF) membrane (Bio-Rad Laboratories; USA) for western blotting in transfer buffer [25 mM Tris, 192 mM glycine (Merck; Germany), 20% methanol (Supelco; Germany)]. Subsequently, the membrane was placed in a blocking buffer [2,5% BSA (Merck; Germany) in PBS-Tween [10 mM PBS, 0.15M NaCl, 0.05% Tween-20 (Sigma-Aldrich; France), pH 7.5] overnight at 4°C.

Presence of PA28α and PA28β was detected with the same primary antibodies as used for intracellular flow cytometry. After washing twice with PBS-Tween, the membranes were incubated at room temperature for one hour in antibody binding buffer [1% BSA in PBS-Tween] that contained either α-PA28α or α-PA28β primary antibodies. The blots were visualised with polyclonal swine anti-rabbit Immunoglobulin HRP secondary antibody (1:5000 dilution; Dako; Denmark) using a SuperSignal West Pico Chemiluminescent substrate kit (Ref.: 34580; Lot No.: UJ2919; Thermo Scientific; USA), which was visualized using a Geldoc Transilluminator with a chemiluminescence detector (Bio-Rad Laboratories; USA).

The protein levels were quantified using ImageJ (bundled with 64-bit Java 1.8.0_172). During the quantification steps, first, the rectangular selections tool from the ImageJ was used to place a box around the first band to analyse. This same rectangle (in terms of height and area covered) was also put around the other bands to analyse as well as on an empty lane to be able to remove background noise from the values later on. Using the straight-line selection tool from the ImageJ toolbar, a line was drawn on the bottom of the corresponding histograms to make it close completely. Next, the wand tool was used to highlight on the areas closed in the previous steps. The percent and area table covering the values from this data was copied to GraphPad. The background value was subtracted from the other values, and these corrected values were statistically analyzed and visualised using GraphPad Prism 9 (nonparametric Mann Whitney test).

2.7 Immunoprecipitation.

To be able to pull down PA28β and possibly its binding partners, NHS-activated magnetic beads (Thermo Scientific Pierce; USA) were coated with anti-PA28β antibodies (identical to the antibodies used in a intracellular flow cytometry staining), according to the protocol provided by the manufacturer.

For the immunoprecipitation itself, around 10 million cells were lysed for 30 min with Pierce lysis buffer [25 mM Tris pH 7.4, 150 mM NaCl, 1% NP-40, 1 mM EDTA, 5% glycerol (Merck; Germany)] at 4°C. After spinning down the lysate (18kg, 30 min, 4°C). Clarified lysate was incubated with 25-50 µL coupled beads overnight. After incubation 500 µL PBS-Tween was used to wash the beads thrice for 20 min at 4°C. Subsequently, elution of the proteins was performed by adding 25 µL 0,1M glycine (pH ~2,0), followed by a 5 min boiling of the sample at 40°C, which in turn was repeated once. For long-term storage, the coupled beads were placed in storage buffer [~138 mM $NaHCO_3$ (Merck, Germany) and ~517 mM NaCl in MQ] supplemented with 0,1-0,05% NaN_3 and stored in the fridge (4°C). Afterwards the beads were stored at -80°C until a western blot was performed.

The elution fraction was further analyzed using SDS the Mini-Protean® TGX™ Precast Gel and western blot as described in paragraph 2.6 (starting from boiling the sample with Laemmli buffer) and the blot was stained against PA28β with the same antibody used in an intracellular flow cytometry staining. Additionally, the elution fraction, 15 µL of used and 15 µL of unused beads were stained with GelCode Blue Stain Reagent (~10-15 mL; Sigma-Aldrich; France) after separation on a Mini-Protean® TGX™ Precast Gel (Bio-Rad Laboratories; USA).

2.8 Statistical analysis.

GraphPad Prism 9 was used to examine the data's significance using a Mann Whitney test (nonparametric), and *p* values <0,05 were considered to be statistically significant. These significance levels were awarded in the following way: *p ≤ 0.05, **p ≤ 0.01.

3. Results.

3.1 IFN-γ stimulation affect expression levels of PA28β, but not that of PA28α.

Both the α and β subunits of PA28αβ are co-ordinately regulated by the immunomodulatory cytokine IFN-γ.[47] To assess to which extend upregulation of both subunits happens in Ana-1 macrophages, I stimulated these cells overnight with 50 ng/µl IFN-γ. I subsequently run the total lysate of both stimulated and unstimulated cells on a western blot and probed it with either anti-PA28α or anti-PA28β antibodies. Immunoblotting with these antibodies resulted in strongly stained bands in all lanes at the molecular weight of ~28 kDa (**Fig. 3a**), which is identical to the predicted molecular masses of both proteins based on their amino acid sequence.

For quantification of the western blot, ImageJ analysis was performed as described in the materials and methods (representative figure of the blocking

around the bands and representative blot is shown in **figure S2**). Protein levels of PA28α were unaffected in response to IFN-γ treatment (p = 0.7373), whereas PA28β levels significantly increased (*p = 0.0280) (**Fig. 3b**).

I further analyzed possible changes in expression levels of both PA28αβ subunits with flow cytometry. Again, Ana-1 macrophages were stimulated as described before, and intracellularly stained with anti-PA28α or anti-PA28β antibodies. I measured the fluorescence of the PE channel (545/566 nm) and compared the mean fluorescent values of each sample with the mean fluorescent value of wildtype Ana-1 cells stained with only the secondary antibody. As visible in **Figure 3c**, there was a slight but insignificant (p = 0.4079) increase in the expression levels of PA28β after stimulation, whereas levels of PA28α remained unaffected (p > 0.9999).

Upregulation of the MHC class I complexes on the surface of the cell due to IFN-γ stimulation has been thoroughly described in literature.[48] To validate the functionality and effectiveness of the stimulation performed in this study, I determined the expression levels of these complexes with an extracellular flow cytometry staining. Therefore, I used a conjugated antibody recognizing the H_2K^b subset of MHC class I complexes in both stimulated and unstimulated cells. The same trend was visible as with the PA28β subunit: MHC class I levels increased due to stimulation (**Fig. 3d**), even though the magnitude of the increase was insignificant (p = 0.1494). Notably, one of three measurements of MHC class I levels had an atypical shape in the corresponding histogram (**Fig. S3c**).

Taking all of the above together, I confirmed that I was working with both PA28α and PA28β. Additionally, overnight IFN-γ stimulation only effected protein levels of the PA28β as confirmed by western blot, whereas flow cytometry analysis showed no significant increase in protein levels of both subunits of PA28αβ and MHC class I complexes at all.

3.2 Inserting a FLAG-tag at the N-terminal site of *Psme1*.

Endogenous affinity tagging allows for identification, immunoprecipitation, and purification of proteins within a cell.[49] To study the docking behaviour of PA28α onto the CP, I intended to endogenously tag PA28α with an affinity tag. For this study I chose to work with the FLAG-tag, considering its small size (8 amino acids) and already has a validated antibody repertoire (e.g. anti-FLAG M2 monoclonal antibody).[50]

The CRISPR/Cas9 system has been used for creating knockouts, knock-ins, and insertion-deletion mutations.[51] This system is targeted to a specific spot on the genome via the recognition of it by sgRNAs, which in turns brings the Cas9 enzyme in close proximity to the DNA. Subsequently, Cas9 introduces a double stranded break which in turn is repaired by a DNA repair system of the cell. There are two main systems: homology directed repair (HDR) and error-prone non-homologous end joining (NHEJ). To be able to precisely insert the FLAG-tag at the N-terminal site of *Psme1*, the HDR pathway needs to be utilized. This

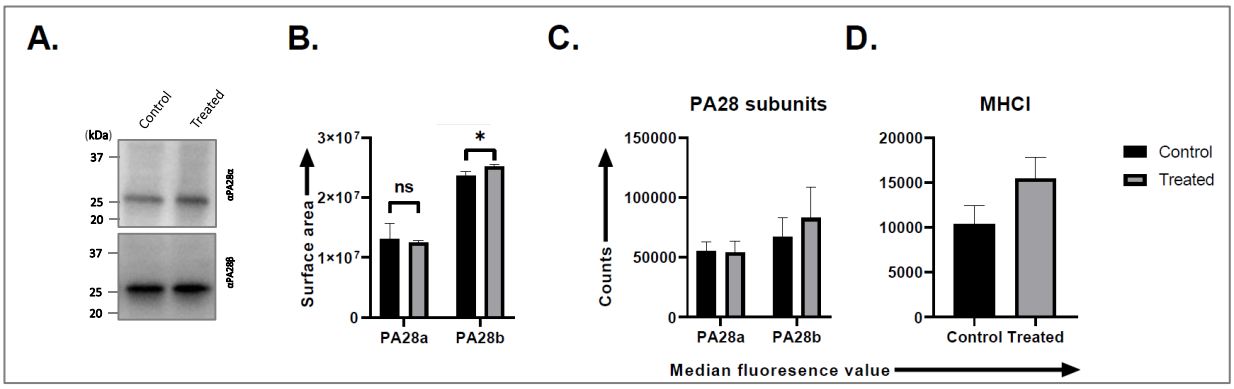

*Figure 3: expression levels of intracellular PA28ϐ and extracellular MHC class I complexes in Ana-1 cells increases after IFN-γ stimulation but is not significant. (A) Western blot analysis of Ana-1 cells before and after stimulation with IFN-γ. PVDF membranes were immunoprecipitated with mAb specific for either PA28α or PA28ϐ. (B) The quantification of A (for all bars n=3). (C) Ana-1 cells stained with either 1:250 dilution anti-PA28α, anti-PA28ϐ mAbs or 1:100 dilution of anti-mouse H-2Kb conjugated mAbs (FITC). Error bars indicate the standard divisions (s.d.) of three individual experiments. Significance was determined via a Mann Whitney (nonparametric) test. Corresponding western blot (**Fig. S3**) and histograms (**Fig. S4**) can be found in the supplementary data.*

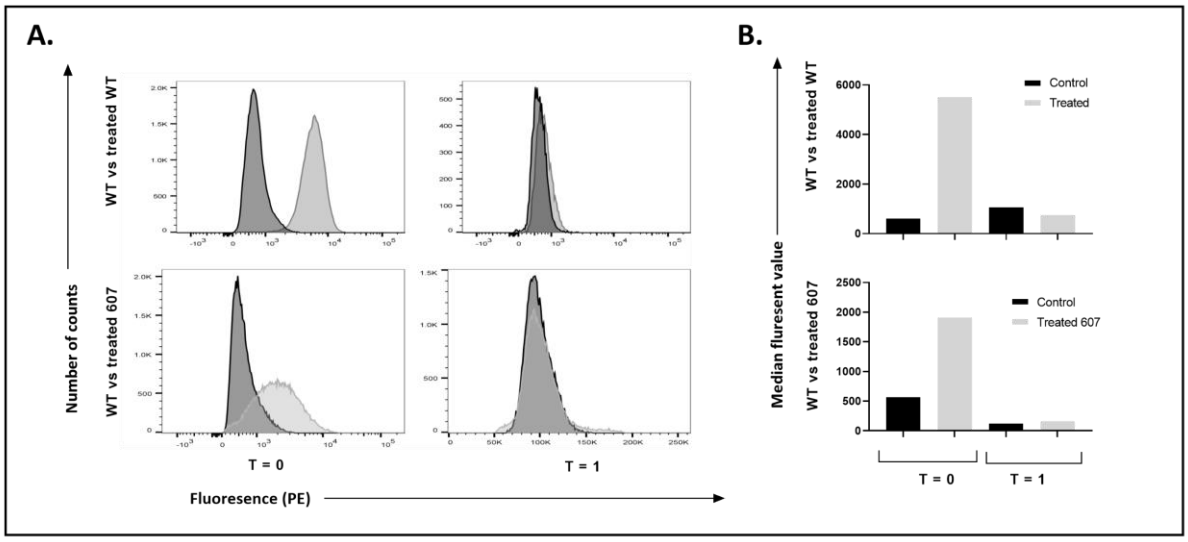

Figure 4: validation of the presence of the FLAG-tag in Ana-1 cell lines two different time points. *(**A**) Ana-1 cells were intracellularly stained against the FLAG-tag and fluorescence of PE was measured with flow cytometry, showing an increase of FLAG expression in T =0. This effect was not seen after a freeze-and-thaw cycle for sample 2, and the 607 Cas9 treated clones. (**B**) the mean fluorescent values of the PE channels. No statistical tests were run on this dataset. Corresponding histograms can be found in the supplementary data (**Fig. S5**). The same gating strategy was used as shown in **figure S4**.*

pathway is under normal circumstances only active during the S/G2 stage of the cell-cycle due to the presence of an extra copy of the DNA. By timely delivery of linear, single stranded DNA in any part of the cell cycle, efficiency of the employment of the HDR pathway increases.[52]

Macrophages are challenging to transfect as almost all established transfection approaches drastically reduce their differentiation and polarization behaviour.[53,54] One way of delivering the CRISPR/Cas9 system (i.e. Cas9- and sgRNA-encoding plasmids & a corresponding single stranded HDR template) into the cells, is electroporation-mediated plasmid DNA delivery.[55] To validate that this method could be used with the murine Ana-1 macrophages of this study, I performed electroporation with an eGFP-encoding plasmid. After ~28 hours eGFP expression was visualized using light microscopy. eGFP was expressed in less than 1% of the viable cell population (empirical data; **Fig. S6**), proving the method of delivery to be successful, despite low efficiency.

After validating that the aforementioned delivery method could be used for delivering plasmids into Ana-1 cells, I moved on to a cell population which were already treated in a preceding study with a Cas9- and sgRNA-encoding plasmids targeting the N-terminal site of *Psme1* (i.e. the gene encoding for PA28α) and the corresponding HDR template to insert the FLAG-tag. First, I put the cells through a serial dilution process, and were only upscaled if the population consisted out of 5-10 different cells initially. After the upscaling steps were completed, insertion of the FLAG-tag was confirmed via an intracellular antibody staining followed by flow cytometry analysis, using the M2 anti-FLAG monoclonal antibody. As depicted in **Figure 4** (**Fig. S5**), at the time of the first measurement (T=0), a sample out the serial dilution step showed FLAG expression in ~99% of the cell population, based on the gating strategy (**Fig. S5a**). This value dropped to ~0% after a freezing, thawing and upscaling cycle (T=1).

As mentioned before, PA28αβ consists out of two different subunits: PA28α and PA28β. In a variety of pathways, there has been evidence that a pathway can sometimes (partially) compensate for the loss of one of its subunits by (over)expressing the other.[56–58] To ensure results out of this study were not due to any compensational mechanism, I also intended to insert the FLAG-tag in a ΔPA28β Ana-1 cell line. Therefore, cells lacking the PA28β subunit were treated with the CRISPR/Cas9 components targeting the N-terminal site of *Psme1* and were afterwards selected for internalization of the sgRNA-encoding plasmid due to electroporation with antibiotics. The viable cells were upscaled, put in serial dilution and analyzed as described before. Between T=0 and T=1 the cells dropped from ~75% FLAG expression within the population to ~0% (**Fig. 4**).

Therefore, I concluded that HDR-driven Cas9 treatment can be applied to modifying murine macrophages, but that several optimisation steps are still required.

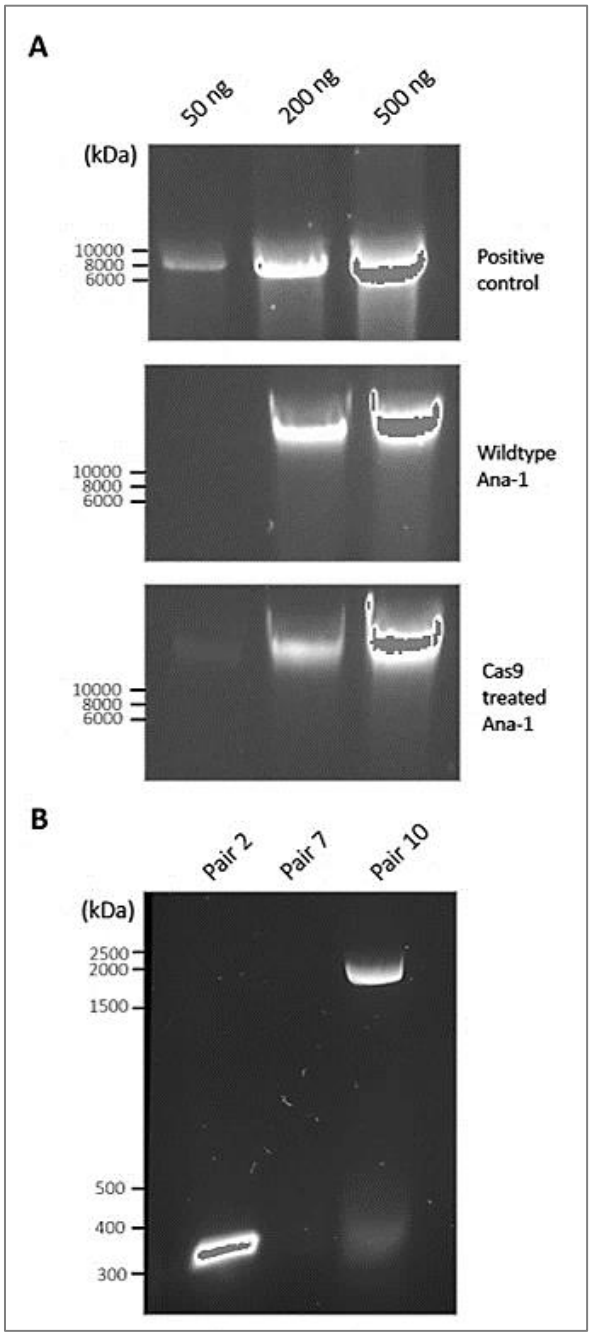

Figure 5: optimisation steps during genotyping. In (a) genomic extraction was performed using a kit and the provided instructions. Subsequently a PCR reaction as run using Q5 as the enzyme for each primer pair, whereafter 15 µL of the PCR product was loaded on the agar gel. In (b) an LR reaction was performed using the NRU1 enzyme. Full figures can be found in supplementary data (Fig. S7 & S8).

3.3 Determining functionality of sgRNAs targeting the C-terminal site of *Psme1*.

Docking of PA28αβ largely depends on the last carboxyl-terminal tyrosine of PA28α (referred to as 249Y). [6,33,34] Another factor possibly playing a role in functional docking is phosphorylation of this tyrosine (referred to as 249Y). Therefore, I intended to mutate the 249Y to have different phosphorylation probabilities (i.e. constantly, on no occasion or occasionally) to study the process of functional docking under different phosphorylation statuses. To modify this amino acid, I chose to again utilize the CRISPR/Cas9 system. First, I validated the functionality of the sgRNAs designed in this study by triggering the error-prone NHEJ repair pathway by only performing the electroporation protocol with the Cas9- and sgRNA-encoding plasmid; so, lacking the HDR template. This usually results in a heterogenous pool of insertions and deletions, which could be analyzed using genotyping in a proceeding study.

The sgRNAs targeting either 249Y or 239K, which would be involved in bringing the Cas9 enzyme in close proximity to the target site, were designed using the Benchling database. Due to the short lifespan of sgRNAs within the cell and to increase efficiency, I chose to order the sgRNAs as primers, including overhangs to ensure placement within the cassettes of the concatemer (Fig. S1). These primers were annealed to form guide RNAs (gRNAs) and were subsequently placed into the concatemer plasmid via golden gate cloning. This cloning technique makes use of repetitive digestion and ligation cycles to place the guides into a cassette. Correct insertion of the gRNAs was validated using sanger sequencing (Fig. S9).

After I performed the electroporation protocol (without providing an HDR template), I extracted genomic DNA from both wildtype cells and the treated cells. I evaluated the absorbance around 280 nm with nanodrop, and confirmed it was genomic DNA by running a digestion reaction with 50 ng, 200 ng and 500 ng as a starting concentration, which was resolved on a 1% agarose gel. As visible in figure 5a, both band thickness and intensity of the bands increases with increasing starting concentrations. In the 50 ng lanes, a clear band is visible for the positive control and a faint one for the treated cells, whereas in wildtype Ana-1 cells no band showed up. The lanes with 200 and 500 ng as a starting concentration of genomic DNA showed clear bands in all conditions, even though

the 500 ng lane is oversaturated compared to the 200 ng lanes. To lower the chance of aspecific products when purified from the gel, I chose the starting concentration with the lowest intensity and that was present in all lanes: 200 ng.

The next optimisation step comprises the PCR conditions. This step is important to amplify the last part of *Psme1* to be able to see if modifications were introduced later on. The primers for the PCR reaction were designed using the NCBI database (primer-blast). Even though this database predicts a primer pair is presumably functional, in real-life this may not always be the case. Therefore, I ordered three different pairs (**Tab. 3**), which all amplify the target site of the sgRNAs, and were all of different lengths. The PCR reaction was run in wildtype Ana-1 cells and the product was resolved on a 1% agarose gel. Primer pair 7 consistently did not show any product on the gel, whereas pair 10 showed bands at the expected heigh of ~1900 (**Fig. 5b**) in 80% of the runs (data not shown). Primer pair 2 showed bands at the expected height of ~338 kDa (**Fig. 5b**) all the time (data not shown).

To study if the electroporation treatment resulted in small genetic variations around the target site, I started the genotyping protocol. For this I run a PCR reaction, using 200 ng of genomic DNA of wildtype and treated Ana-1 cells and primer pair 2. The product was resolved on a 1% agarose gel, and corresponding bands were cut out, purified and handed in for sequencing by Macrogen. I did not perform analysis of the sequencing results in this study due to time constraints.

In this study, I confirmed I extracted DNA from WT and treated cells and optimised several parts of the PCR protocol: starting concentration of genomic DNA and the primer pair to use.

3.4 Immunoprecipitation of PA28β needs additional optimisation steps.

As mentioned before, an affinity tag can be used to immunoprecipitate proteins within the cell to study their behaviour. In this method, magnetic beads are coupled to antibodies which specifically recognizes a protein. After an incubation period with lysate the antibodies are supposed to be bound to the protein of interest. The beads can subsequently be removed out of the lysate by using a magnetic stand.

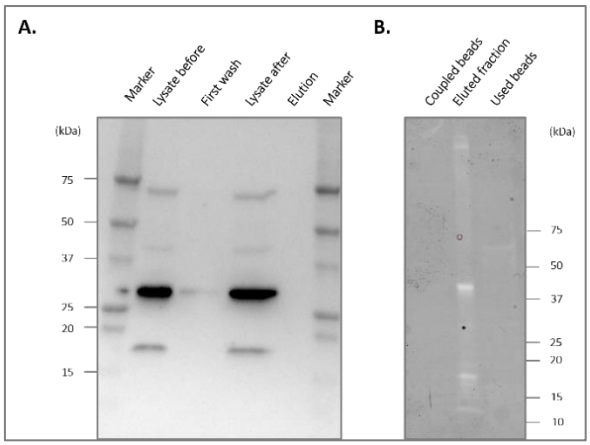

*Figure 6: western blot analysis and Coomassie staining. Each lane was loaded with Ana-1 lysate, electrophoresed on an SDS-PAGE gel and transferred to a polyvinylidene difluoride membrane. Primary antibody used for protein detection are specific for rabbit PA28β, and secondary is specific for rabbit-antibodies. Full western blot and Coomassie stained blot can be found in supplementary data (**Fig. S10 & S11**).*

In this study I wanted to use this method to pull down FLAG-tagged PA28α to study its docking behaviour. However, while FLAG-insertion was still an ongoing procedure, I chose to pull for PA28β during optimisation steps of this immunoprecipitation protocol. Building on the finding that PA28β showed more strongly stained bands on western blots (data not shown, example can be found in **figure 3a**).

I started with coupling the beads to antibodies that specifically recognize PA28β. Therefore, I activated them with acid and incubated them overnight with anti-PA28β polyclonal antibodies. Validation of the coupling procedure was not performed in this study. After coupling of the beads, I incubated them overnight with lysate of wildtype Ana-1 cells. All proteins the beads captured during this period were eluted and used in a western blot.

As depicted in **figure 6a**, immunoblotting with anti-PA28β antibodies resulted in strongly stained bands at the expected weight of PA28β (~28 kD) in both the lysate before and after. In other words, before and after the beads were added and subsequently removed, there were PA28β subunits present. Furthermore, in the same lanes there are three aspecific bands visible which cannot be explained. Additionally, in the first wash of the beads a faint band is visible at the same height as PA28β, even though this is presumably spill over from the adjacent lane,

considering there is a similar band at the same height in the lane of the marker that should not be there. The elution fraction doesn't show any bands.

Next, a Coomassie Blue staining was run to 1) validate whether all captured proteins were eluted from the beads and 2) if there are proteins in the elution fraction that possibly did not show up on the western blot. The lanes of the coupled, unused beads and the beads used in the pull-down protocol showed no bands, whereas the eluted fraction showed several bands which corresponds to the aspecific bands visible in the western blot (lysate before and after adding the beads)

Considering the findings above, several optimisation steps are needed before a proceeding study can utilize a magnetic pull down to study the docking behaviour of PA28α.

4. Discussion.

The current study mainly focussed on the underlying mechanism of the involvement of phosphorylation in functional docking of PA28α onto the proteasomal core. It is already described in literature that PA28α ensures docking onto the CP predominantly with the last carboxyl-terminal tyrosine, [6,33,34] but that is not enough to activate the hydrolytic activities of the CP. [30] Therefore, I focussed on optimising several protocols to study 1) the physical interaction between PA28α and the CP and 2) its subsequent effect on antigen presentation in cells with different phosphorylation probabilities on the last carboxyl-terminal tyrosine of PA28α. Even though the full question remains to be answered, the progress on the optimisation steps will be discussed here.

4.1 The effect of interferon-γ on expression levels of both PA28α and PA28β in wildtype Ana-1 cells.

The major inflammatory cytokine IFN-γ is known to influence a broad range of pathways within the cell,[59–61] bringing it to a "viral-protective" state, and among others, results in the upregulation of both PA28αβ subunits.[10,62,63] This report is inconsistent with the finding that neither PA28α nor PA28β showed a significant change between expression levels due to stimulation in flow cytometry analysis (**Fig. 3c**). Interestingly, western blot analysis did show a significant upregulation of the β-subunit of PA28αβ alone (**Fig. 3b**). These conflicted results require follow up experiments using a higher sample size to ensure these significant results were not due to an outlier or systemic fault.

Based on the finding that stimulation did not result in enhanced MHC class I expression either (**Fig. 3c**), the question arises to which extend stimulation succeeded. Especially taken the fact that MHC class I upregulation due to interferon is well described in literature.[48] A possible explanation could be that the biological activity of the IFN-γ stock used has declined due to repeated freeze-and-thaw cycles. Even though IFN-γ has proven to be quite stable in repeated freeze-and-thaw cycles, it has generally been measured in 5 of these cycles,[64] which is remarkably lower than the number of cycles the stock used went through. Another explanation could be that the cells were already stimulated by self-produced interferon-gamma, and the supplied IFN-γ did not have any additional effects. This is not unlikely, since Ana-1 cells, which are murine macrophages, are known to produce IFN-γ themselves,[65] if activated. Nevertheless, it should be noted that the sample size of determining the MHC class I levels before and after stimulation is extremely low (n=2), which is technically too low to determine p-values. This statement is supported by the fact that out of the two measurements for MHC class I staining after stimulation, the histogram shows an aberrant shape, two peaks instead of one (**Fig. S4**), which massively impacts the p-value.

To check for both the effectiveness and functionality of the used IFN-γ, I suggest redoing the experiments and run along an enzyme-linked immunosorbent assay (ELISA) to check for presence of IFN-γ in unstimulated cells and to also use another cell type which cannot produce IFN-γ, but can respond to it, to examine if the IFN-γ stock still has biological activity, and to use a bigger sample size for quantification.

4.2 Utilizing the CRISPR/Cas9 system to modify the genes encoding for both PA28α and PA28β.

The CRISPR/Cas9 system, originating from the prokaryotic adaptive immune system, for genome editing (GE) has revolutionized the field of modern molecular biology for several years.[66] The CRISPR/Cas9 system has been used for creating knock-outs, knock-ins and insertion-deletion mutations.[51] A long-standing physical method for delivery of the components of this

system is electroporation-mediated plasmid DNA delivery.[55] This technique utilizes pulsed electrical currents to transiently open pores in the cellular membrane, allowing for small components to flow into the cell. This study made use of the CRISPR/Cas9 system to trigger two different repair pathways (i.e. HDR and NHEJ) within the cell with three different purposes.

4.2.1 Knocking out PA28(α)β utilizing error prone DNA repair.

To study the impact of a protein and acquire knowledge about the functions of it, often a knockout study is performed. Usually, the protein of interest is knocked out alone, or one of its most important binding partners. In this study, I wanted to work with several variants of Ana-1 macrophages: 1) wildtype Ana-1 cells as a negative control, 2) complete PA28αβ knockout Ana-1 cells to work out the lack of the protein of interest and 3) a Ana-1 cell line lacking the PA28β subunit to validate for any compensational mechanism.

In several biological pathways, there has been evidence that a pathway can sometimes (partially) compensate for the loss of one of its subunit by (over)expressing the other.[56–58] It is already established that both the PA28 subunits have differentially regulated gene expression,[67] and that *in vitro*, isolated PA28β subunits, forming homoheptamers, are unable to form a complex with stimulatory activity,[20,68] suggesting this subunit enhances the functionality of the alpha-subunit or has other functions within the cell and lowering the chances of a compensational mechanism in case of losage of either one of the subunits.[6] Nevertheless, there also have been notions of a homoheptamer of the β-subunit being able to stimulate the hydrolytic capacity of the core particle or at least can associate with it.[69,70] To make sure any outcome of this line of study were not due to any compensational mechanism, I chose to not only work with a wildtype and ΔPA28α Ana-1 cell line, but also a ΔPA28β Ana-1 cell line. Nevertheless, it is not unlikely that removal of the β-subunit could be of influence on the results in a proceeding study. *In vivo* studies already showed that inhibition of the β-subunit of PA28αβ resulted in cells that lacked immunoproteasomes, showed defects in the cytotoxic T- lymphocyte responses to the choriomeningitis virus and the cells were unable to present the PA28 enhanced $OVA_{257-264}$ epitope, which is also known as the SIINFEKL peptide.[71] Therefore, it would be beneficial to compare wildtype and ΔPA28αβ Ana-1 cells with cells lacking the PA28β subunit by at least looking at the general response to (bacterial or viral) infection, MHC class I and II expression levels and possible changes in PA28αβ dependent antigen presentation. When it could be taken to *in vivo* studies, improving our understanding of the functionality of PA28β is of importance before targeting PA28α *in vivo* to prevent deleterious or harmful effects.

The ΔPA28β Ana-1 cell line was provided by M. Wawrzyniuk, in which the CRISPR/Cas9 system was utilized to trigger the non-homologous end joining (NHEJ) pathway of DNA repair (i.e. error prone). In this study, the validation steps were not performed again.

4.2.2 Inserting an affinity tag in front of Psme1 utilizing the HDR pathway of the cells.

The second way the CRISPR/Cas9 system was employed was to trigger the HDR DNA repair pathway (i.e. specifically mutating a genome segment) to insert an affinity tag in front of *Psme1* in both wildtype cells and the aforementioned PA28β knockout. Endogenous affinity tagging allows for identification, modification, production, isolation, and purification of proteins within a cell.[49] Most affinity-tag systems are applicable to a variety of different proteins, are easy and specific to remove and hardly have effect on tertiary structure and biological activity within the cell.[72] Therefore, these tags have become widespread a lot of areas of research. One of the most commonly used small peptide tags is the FLAG-tag.[73] Therefore, this study proceeded in creating a cell line in which the protein of interest (i.e. PA28α) would be N-terminally tagged with this affinity tag.

A previous study of L.G. Masselink (2020)[37] already started optimising the usage of the CRISPR/Cas9 system to insert this affinity tag at the N-terminal site of *Psme1*, since the C-terminal site is involved in the docking and activating of the 20S CP.[35] Therefore, placing it C-terminally would probably interfere too much with the biological activity of PA28α. This study obtained a mix of cells of the previous study,[37] which were a mix between wildtype Ana-1 cells and genetically targeted Ana-1 cells (i.e. cells which potentially expressed the FLAG tag). This mix was upscaled, and a sample of it was intracellularly stained against FLAG and fluorescence was measured using flow cytometry. Additionally, I chose to insert the FLAG-tag at the N-terminal site of *Psme1* in Ana-1

ΔPA28β cells, following the procedure described by L.G. Masselink (2020).[37]

Flow cytometry analysis showed that expression of the FLAG-tag intracellularly was present after electroporation at timepoint 1 (**Fig. 4**). However, the second time, after a freeze-thaw-upscale cycle, expression of the tag went to zero for both the treated WT and the treated Ana-1 ΔPA28β cells (a.k.a. 607 clone).

One probability for the "losage" of the tag in the cells I cared for could be due to my inexperience with cell culture, meaning I presumably either switched WT with Cas9 treated cells or contaminated the two somewhere during culturing. This hypothesis is supported by the fact that treated cells handled by M. Wawrzyniuk did contain FLAG after a freezing-thawing cycle (data not shown). Nevertheless, it should be noted that the expression level of FLAG in the population stained dropped immensely. Another possibility is that cells which are not genetically engineered have a shorter replication cycle (empirical data not shown) or that these cells are less likely to survive a freeze-and-thawing cycle and therefore WT cells could possibly outgrow the engineered cells. However, there is no substantial prove to support this claim.

4.2.3 Modifying phosphorylation probability of the last carboxyl-terminal amino acid in PA28α.

As a third and final way the CRISPR/Cas9 system was used to target the Cas9 enzyme to the last C-terminal tyrosine (249Y) of *Psme1* with the intention to mutating it in a proceeding study. The three different mutations planned were to mutate the last carboxyl-terminal tyrosine of PA28α and to change the 238K to a stop codon to remove the disordered segment at the C-terminal side.

I showed that the usage of the sgRNA designed to remove the tail, resulted in cells unable to grow and divide after the electroporation treatment (data not shown). It could be that the sgRNA targeted not only the *Psme1* gene, but also other important parts of the genome. Even though this is questionable, considering the low off-score is predominantly due to a pseudogene, which are relatively rare reinsertions of mRNA of functional genes into the genome but lack un upstream promotor sequence and are therefore transcriptionally inactive.[74] Therefore, mutated sections of this pseudogene would unlikely result in changed viability. Moreover, since PA28αβ has been proven to be involved in degradation of oxidised proteins, a knock-out of either one or two of the PA28 subunits impairs tolerance to oxidative stress.[75] Especially since, during oxidative stress, the 26S proteasome gets inactivated, thereby lowering the amount of functional proteasomal particles, and if PA28 is not present, or functional, cells are more prone to damage to the DNA and other important molecules which could ultimately even lead to apoptosis.[76] Hence, a possibility arising is that the guides did work, but resulted in cells in which the *Psme1* was rendered unfunctional (e.g. stop codon was removed), and that due to either electroporation or the antibody selecting process the oxidative stress levels were excessively high, and could not be handled by the cells anymore.

In any way, it is still important for future research to reconfirm that the tail of PA28α is indeed involved in its docking mechanism onto the CP. One way to proceed is to use another possible sgRNA to target the disordered carboxyl-terminal segment. For the designing of the sgRNAs I used the website Benchling, which is a database which undergoes updates continuously. When at the end of this study (Benchling version 2021_09) the values of the sgRNAs designed were checked, I found several additional sgRNAs coming up compared to the ones I found at the beginning of this study. One of the provided possibilities for removing the last disordered segment of PA28α had a more favourable on-score compared to the one we used in this study. This option cuts at position 56200188 at the positive strand (sequence GAGAAGCTCAAGAAGCCCCG) with on- and off-scores of 53.2 and 25.3, respectively. The lower off score is due to chromosome 1 (confirmed pseudogene) and 15 (presumably non-coding DNA) Since the on-score is 76,7% higher compared to the sgRNA value used, so presumed binding affinity of this guide is higher. Therefore, I suggest redoing the experiment with a newly designed guide.

Electroporation-mediated plasmid DNA delivery treatment with the sgRNA targeting 249Y and a Cas9 encoding plasmid did result in cells being able to grow. The idea behind using error prone DNA repair was that with genotyping small genetic changes should become visible around the target site if the used sgRNA were functional. First, DNA was extracted from both wildtype and Cas9 treated Ana-1 cells, and via the absorbance the concentration was determined. This genomic DNA was run in a digestion reaction, which

results in the genome being cut at several places. I found that using 200 ng of starting concentration of DNA resulted in bands in both wildtype and Cas9 treated Ana-1 cells while not being oversaturated (**Fig. 5a**). The fact that in increasing concentrations the band thickness increases, supports the fact indeed genomic DNA was loaded onto the gel. Using the 200 ng of genomic DNA as a starting concentration, the primers designed with the NCBI primer blast tool were run in a PCR reaction (**Fig. 5b**). One of the primer pairs was not able to amplify the last exon of *Psme1*. One of the remaining pairs did result in clean bands on the agarose gel, but was, however, not able to amplify the genome in 100% of the runs, whereas the last pair (pair 2) was able to do that. Therefore, I decided to continue with the 200 ng starting concentration of the genomic DNA and primer pair 2 for amplifying the last exon of *Psme1*. The setting of the Thermocycler during the PCR reaction was not optimised in this study yet, which should be looked at in a proceeding study.

After the optimisation of several steps of the genotyping protocol, a sequencing reaction by Macrogen (Netherlands) was performed to validate if the CRISPR/Cas9 system was successful in inducing mutations around the target site. However, due to time constraints this analysis was not finalized in this study.

4.3 Monitoring differences between wildtype and Cas9 treated Ana1 cells.

If the sgRNAs in this study target the Cas9 enzyme around the target site (i.e. the carboxyl-terminal end of *Psme*1), and the mutants with different phosphorylation probabilities on this last amino acid are created, the next step is to readout the differences between the mutants. The main objective of this study was to find out if the phosphorylation probability of the last carboxyl-terminal tyrosine of PA28α is used as a regulatory mechanism for docking onto the CP. To see if the phosphorylation level changes, I started to optimise an immunoprecipitation protocol: NHS magnetic pull down. Another way to monitor if PA28 functionally docks, is to look at the presentation of a PA28αβ enhanced antigen (not performed in this study).

4.3.1 Immunoprecipitation of PA28β.

To my knowledge, previous studies have predominantly worked with different kind of agarose beads during immunoprecipitation steps in similar experiments.[37,77] Working with these types of beads requires several technical skills, since it is extremely difficult to thoroughly remove the buffer during washing steps without disturbing some of the pelleted beads. This particular disadvantage is taken away with using magnetic beads, since all the beads that presumably captured the target protein are held to the side of the tube, making removal of the fluids straightforward.

This study made a start of optimising the NHS magnetic pull-down protocol for Ana1 macrophages. Due to fact no FLAG containing Ana-1 cell line has been generated yet, I chose to couple the beads with antibodies specific for PA28β. Considering the fact that all western blots showed strongly stained bands for PA28β (data not shown), which could have made optimisation of this protocol more easily.

During optimisation rounds I found that efficiency of the protocol was extremely low without optimisation steps. None of the western blots showed any bands at the expected height of either PA28α or PA28β in the elution fractions (data not shown). This could be due to several reasons: 1) coupling of the beads was unsuccessful, 2) the proteins bound during incubation period were not eluted from the beads or 3) target protein was not present in the cells.

Both western blots (**Fig. 3a & 6a**) and flow cytometry (**Fig. 3c**) analysis show strongly stained bands at the expected height of both PA28α and PA28β. Therefore, the third reason was determined invalid. Furthermore, the Coomassie blue staining of a small number of beads used in the pull-down protocol did not show any bands at the expected heights. This staining stains proteins aspecific, making it highly unlikely that there was still PA28β bound to the beads. Concludingly, presumably the beads were not correctly coupled to antibodies. This can either mean the antibodies were not bound at all or bound in a way that rendering their functionality close to or even reaching zero.

Coupling efficiency of the antibodies to the beads can vary due to a variety of reasons. First of al, since the concentration of the antibody was not optimised in this study, there is a possibility that either a too high or too low concentration was added which could deteriorate coupling efficiency. Second, it could have been that the primary amine-containing buffer was not completely removed before the coupling procedure. Therefore, I suggest for future research to increase the amount of dialyze or desalting the antibody to completely remove the Tris and glycine

possible present in the mixture and to make all buffers from scratch. If both coupling and pulling down PA28β succeeds in the future, it would be beneficial to still continue to optimise the protocol even further for pulling for PA28α or the FLAG-tagged PA28α variant to see possible changes if the phosphorylation probability of 249Y is changed or in cells in which the β-subunit of PA28αβ is knocked out.

Even though only in lysate before and after there are bands at the expected height of PA28β, there are also some bands visible in both the western blot and the Coomassie stained blot at other heights. The bands in both blots are at around the same height and cannot be explained other than it being background or contamination. Additionally, there seems to be a band in the washes lane, giving rise to the possibility the proteins captured during incubation are washed off due to too harsh wash conditions. However, it is only at one side of the lane and is most likely spill over from the lane next to it (lysate before). This claim is supported by the fact that also in the marker lane a small band is visible which is only present at the right side of the lane (i.e. the side the lysate before lane is located). Until now, all the fluid from the washes was collected in the same Eppendorf and run on a western blot, whereas in this run only the first wash was loaded due to contamination of the other two washes. Future research should look into the possibility the protein is eluted in the wash steps. I suggest starting with validating if the coupling of the beads was successful, by using a more sensitive blot to confirm whether or not antibodies are coupled to it, for example a silver staining.

4.3.2 Antigen presentation monitoring of a PA28αβ enhanced peptide.

Functional docking of PA28αβ is composed of two different mechanisms. It comprises both the physical interaction between the two proteins, and subsequently or at the same time the change in functionality of one of them, which is in this case the core particle. It is important to be reminded of this, since the mutants designed in this study could possibly still dock onto the core particle, but could be incapable of stimulating the hydrolytic capacity of the CP. Therefore, it is not only important to look at if the proteins dock on each other, but also to the subsequent (expected) effect.

Considering the involvement of PA28αβ in the antigen processing pathway, [25–28] it would be beneficial to look at possible changes in antigen presentation of an PA28αβ enhanced antigen. A well described peptide for this is the SIINFEKL-peptide, or pOVA, which already has a validated antibody repertoire.[71] Changes in antigen presentation of SIINFEKL can be measured using either flow cytometry in the same way as performed in this study (i.e. only using another antibody and concentrations of it), or a B3Z assay. A B3Z assay contains a T-cell hybridoma which cells are specifically engineered to recognise the SIINFEKL epitope in context of H-2Kb (i.e. the MHC class I subtype present in Ana1 macrophages). Since both PA28α and -β are supposed to be upregulated by IFN-γ, I propose to do all these experiments with both stimulated and unstimulated cells to see if the changes are proportional to ensure that if docking happens, also the functionality of the docking is present, or not.

4.4 Future perspective.

If in proceeding studies it could be confirmed that phosphorylation of the last carboxyl-terminal tyrosine is indeed involved in regulating the docking propensity of PA28α, the subsequent question arising is which kinase is involved in this pathway. Identifying the right tyrosine-kinase could be of major importance before we would be able to modulate PA28α's activity in pathologies involving aberrant functionality of either PA28α or PA28αβ. It is not unlikely that, if phosphorylation is indeed involved, the yet unidentified kinase is linked to the Jak/STAT-1 pathway.[78] First of all, this pathway is triggered by stimulation with IFN-γ and upregulates the expression of both PA28α and PA28β.[14,63,79] Moreover, IFN-γ stimulation is already known to change the phosphorylation pattern of both the proteolytic core, [80] PA28α, and PA28β,[37] as well as proteins associated with proteasomal function.[80]

Another pathway this kinase could play a role in is the nuclear factor (erythroid-derived 2)-like 2 (Nrf2) signal transduction pathway. It has already been demonstrated that this pathway, which controls the expression of an array of antioxidant response-element-dependent genes, couples the 20S core particle and PA28αβ to the oxidative stress response.[81] Oxidised proteins are mainly degraded by proteasomes in an ATP-independent and ubiquitin-independent manner,[82] thereby excluding the 26S proteasome (i.e., 19S regulatory particle docked onto the 20S CP). Hence, there is a likelihood that the unidentified kinase

is both in the Jak/STAT-1 pathway as in the Nrf2 signal transduction pathways.

Understanding which kinase is possibly involved in this pathway is essential before we can target it specifically for therapy. As mentioned before, aberrant levels of PA28α have been seen in a variety of different pathologies, including several different types of cancers,[38–43] insulin resistance,[83] and diabetic nephropathy.[84,85] According to the needs of the situation, docking propensity could be either enhanced or repressed according to the needs of the situation. Taking the example of PA28αs involvement in oxidative stress could be used as a therapeutic target against oxidised proteins, which accumulate during, for example, ageing and several neurodegenerative diseases (e.g. Alzheimer's disease and Parkinson's disease).[86] Nevertheless, due to the fact that many kinases have a multitude of substrates, and both the Jak/STAT-1 and the Nrf2 pathways are quite general, and involved in many different interactions, targeting this kinase can result in a variety of side effects *in vivo*. Therefore, if the side effects are too problematic, it is presumably more beneficial to target PA28α itself. There are several protein inhibitors which block the interaction between the isolated proteasome and PA28αβ, including PI31,[87] HIV-1 Tat protein,[88] and the Hepatitis B Hbx peptide.[89] Except the latter option, these inhibitors also impair catalytic capacity of the CP. Therefore, more research is required to determine the usability of targeting the docking site directly *in vivo*.

On the other hand, if phosphorylation of the last carboxyl-terminal tyrosine turns out not to be involved in the regulation of the docking propensity of PA28α in a cellular context, it is still worth determining the reason behind the changed phosphorylation pattern of PA28αβ after stimulation with IFN-γ, and how it is linked to proteasome activation. A study by Li, Lera and Etlinger (1996) already showed that after dephosphorylation with alkaline phosphatases, PA28αβ is incapable of activating the CP's hydrolysis.[34] However, as mentioned before, docking onto the core, and activating it are two different processes. Therefore, even if it is not involved in the docking itself, it can still influence the whole process on another level. For example, changing the phosphorylation status of specific residues can possibly be of influence in substrate selection. A higher level of phosphorylated residues could allow for smaller, more hydrophilic epitopes to diffuse in and out of the CP, while more hydrophobic epitopes are retained longer for longer, resulting in more peptides being released, ticking the boxes for being an antigenic peptide. Hence, it can be beneficial to pinpoint which residues have changed phosphorylation patterns after IFN-γ stimulation by, for example, phosphorylation analysis (e.g., mass spectrometry). Besides, even if the process of changing the phosphorylation pattern does not happen *in vitro* and *in vivo*, it could still be utilized in therapy to modify this pathway in later stages of research.

4.5 Conclusion.

Even though this study did not manage to completely answer the main question initially asked, it is still worth it for future research to continue this line of research. Modulating the degradational activity of the proteasomal system by targeting PA28α proteins therefore offers a suitable candidate for the development of novel, mechanism-based therapeutic modalities for pathologies (e.g. several types of cancer)[84,85] involving aberrant functionality of either PA28α or PA28αβ or when changed functionality could be beneficial.

Ultimately, several lines of study are showing PA28αβ participating in MHC class I antigen presentation, protein degradation, cellular stress resistance, [16,81,90] protein damage control during early embryogenesis,[38] cell adhesion,[39] regulating cancer cell growth & proliferation,[42,91] and even a chaperone-like function has been reported.[38] Even though the underlying molecular mechanisms still require further investigation, it emphasises the wide arrange of pathways PA28α participates in. A potential target point for therapy could be the interplay between the proteasomal core and PA28αβ. Therefore, increasing the knowledge surrounding the functional docking of this cap could prove of major importance. This study in particular focused on optimising several toolsets to look answer the question of phosphorylation of a single amino acid residue at the carboxyl terminus of the PA28α subunits is used as a regulatory mechanism for docking onto the 20S proteolytic core in murine macrophages.

5. Acknowledgements.

I want to express my gratitude for a whole amount of people who made internship both amazing to be in and extremely helpful for developing several skills career wise. First of all, I give my thanks to Lena,

for guiding me through this whole project, being patient when I asked so many questions and that she showed me how to move through the research question and how to shape the experiments around it. Secondly, I want to thank both my examiners, Alice Sijts and Bertrand Kleizen for their time and willingness to help me. Third, I want to show my appreciation for everyone on the lab, but most of all my PI group, for helping me move through the day, find everything I needed and showing me how to perform analysis for every single technique I struggled through. Not to forget Fatemeh Pashaie for providing both the protocol and recourses for a positive control I desperately needed or C. Konrdörfer Rangel for showing how to do a quantitative western blot analysis in her own time in between her exams. Lastly, I want to thank the whole department for their time, money, and fruitful discussions during lunch and anytime I needed it, and especially Jacco, who had to endure every long waiting step alongside me.

6. References.

1. Muñoz, C., San Francisco, J., Gutiérrez, B., & González, J. (2015). Role of the Ubiquitin-Proteasome Systems in the Biology and Virulence of Protozoan Parasites. BioMed research international, 2015, 141526. https://doi.org/10.1155/2015/141526
2. Adams J. (2003). The proteasome: structure, function, and role in the cell. Cancer treatment reviews, 29 Suppl 1, 3–9. https://doi.org/10.1016/s0305-7372(03)00081-1
3. Vigneron, N., & Van den Eynde, B. J. (2014). Proteasome subtypes and regulators in the processing of antigenic peptides presented by class I molecules of the major histocompatibility complex. Biomolecules, 4(4), 994–1025. https://doi.org/10.3390/biom4040994
4. Sijts, E. J., & Kloetzel, P. M. (2011). The role of the proteasome in the generation of MHC class I ligands and immune responses. Cellular and molecular life sciences : CMLS, 68(9), 1491–1502. https://doi.org/10.1007/s00018-011-0657-y
5. da Fonseca, P. C., & Morris, E. P. (2015). Cryo-EM reveals the conformation of a substrate analogue in the human 20S proteasome core. Nature communications, 6, 7573. https://doi.org/10.1038/ncomms8573
6. Song, X., von Kampen, J., Slaughter, C. A., & DeMartino, G. N. (1997). Relative functions of the alpha and beta subunits of the proteasome activator, PA28. The Journal of biological chemistry, 272(44), 27994–28000. https://doi.org/10.1074/jbc.272.44.27994
7. Murata, S., Yashiroda, H., & Tanaka, K. (2009). Molecular mechanisms of proteasome assembly. Nature reviews. Molecular cell biology, 10(2), 104–115. https://doi.org/10.1038/nrm2630
8. Kammerl, I. E., & Meiners, S. (2016). Proteasome function shapes innate and adaptive immune responses. American journal of physiology. Lung cellular and molecular physiology, 311(2), L328–L336. https://doi.org/10.1152/ajplung.00156.2016
9. Kasahara M. (2021). Role of immunoproteasomes and thymoproteasomes in health and disease. Pathology international, 71(6), 371–382. https://doi.org/10.1111/pin.13088
10. Fabunmi, R. P., Wigley, W. C., Thomas, P. J., & DeMartino, G. N. (2001). Interferon gamma regulates accumulation of the proteasome activator PA28 and immunoproteasomes at nuclear PML bodies. Journal of cell science, 114(Pt 1), 29–36.
11. Bajorek, M., Finley, D., & Glickman, M. H. (2003). Proteasome disassembly and downregulation is correlated with viability during stationary phase. Current biology: CB, 13(13), 1140–1144. https://doi.org/10.1016/s0960-9822(03)00417-2
12. Yamano, T., Murata, S., Shimbara, N., Tanaka, N., Chiba, T., Tanaka, K., Yui, K., & Udono, H. (2002). Two distinct pathways mediated by PA28 and hsp90 in major histocompatibility complex class I antigen processing. The Journal of experimental medicine, 196(2), 185–196. https://doi.org/10.1084/jem.20011922
13. Stadtmueller, B. M., & Hill, C. P. (2011). Proteasome activators. Molecular cell, 41(1), 8–19. https://doi.org/10.1016/j.molcel.2010.12.020
14. Brooks, P., Fuertes, G., Murray, R. Z., Bose, S., Knecht, E., Rechsteiner, M. C., Hendil, K. B., Tanaka, K., Dyson, J., & Rivett, J. (2000). Subcellular localization of proteasomes and their regulatory complexes in mammalian cells. The Biochemical journal, 346 Pt 1(Pt 1), 155–161.
15. Nandi, D., Tahiliani, P., Kumar, A., & Chandu, D. (2006). The ubiquitin-proteasome system. Journal of biosciences, 31(1), 137–155. https://doi.org/10.1007/BF02705243
16. Pickering, A. M., & Davies, K. J. (2012). Differential roles of proteasome and immunoproteasome regulators Pa28αβ, Pa28γ and Pa200 in the degradation of oxidized proteins. Archives of biochemistry and biophysics, 523(2), 181–190. https://doi.org/10.1016/j.abb.2012.04.018
17. Mott, J. D., Pramanik, B. C., Moomaw, C. R., Afendis, S. J., DeMartino, G. N., & Slaughter, C. A. (1994). PA28, an activator of the 20 S proteasome, is composed of two nonidentical but homologous subunits. The Journal of biological chemistry, 269(50), 31466–31471.
18. Wilk, S., Chen, W. E., & Magnusson, R. P. (1998). Properties of the proteasome activator subunit PA28 alpha and its des-tyrosyl analog. Archives of biochemistry and biophysics, 359(2), 283–290. https://doi.org/10.1006/abbi.1998.0918
19. Ahn, K., Erlander, M., Leturcq, D., Peterson, P. A., Früh, K., & Yang, Y. (1996). In vivo characterization of the proteasome regulator PA28. The Journal of biological chemistry, 271(30), 18237–18242. https://doi.org/10.1074/jbc.271.30.18237
20. Huber, E. M., & Groll, M. (2017). The Mammalian Proteasome Activator PA28 Forms an Asymmetric $\alpha_4\beta_3$ Complex. Structure (London, England : 1993), 25(10), 1473–1480.e3. https://doi.org/10.1016/j.str.2017.07.013
21. Zhang, Z., Krutchinsky, A., Endicott, S., Realini, C., Rechsteiner, M., & Standing, K. G. (1999). Proteasome activator 11S REG or PA28: recombinant REG alpha/REG beta hetero-oligomers are heptamers. Biochemistry, 38(17), 5651–5658. https://doi.org/10.1021/bi990056+
22. Sugiyama, M., Sahashi, H., Kurimoto, E., Takata, S., Yagi, H., Kanai, K., Sakata, E., Minami, Y., Tanaka, K., & Kato, K. (2013). Spatial arrangement and functional role of α subunits of proteasome activator PA28 in hetero-oligomeric form. Biochemical and biophysical research communications, 432(1), 141–145. https://doi.org/10.1016/j.bbrc.2013.01.071
23. Raule, M., Cerruti, F., Benaroudj, N., Migotti, R., Kikuchi, J., Bachi, A., Navon, A., Dittmar, G., & Cascio, P. (2014). PA28αβ reduces size and increases hydrophilicity of 20S

immunoproteasome peptide products. Chemistry & biology, 21(4), 470–480. https://doi.org/10.1016/j.chembiol.2014.02.006

24. Dick, T. P., Ruppert, T., Groettrup, M., Kloetzel, P. M., Kuehn, L., Koszinowski, U. H., Stevanović, S., Schild, H., & Rammensee, H. G. (1996). Coordinated dual cleavages induced by the proteasome regulator PA28 lead to dominant MHC ligands. Cell, 86(2), 253–262. https://doi.org/10.1016/s0092-8674(00)80097-5
25. Rechsteiner, M., Realini, C., & Ustrell, V. (2000). The proteasome activator 11 S REG (PA28) and class I antigen presentation. The Biochemical journal, 345 Pt 1(Pt 1), 1–15.
26. van Hall T, Sijts, A., Camps, M., Offringa, R., Melief, C., Kloetzel, P. M., & Ossendorp, F. (2000). Differential influence on cytotoxic T lymphocyte epitope presentation by controlled expression of either proteasome immunosubunits or PA28. The Journal of experimental medicine, 192(4), 483–494. https://doi.org/10.1084/jem.192.4.483
27. Xie, S. C., Metcalfe, R. D., Hanssen, E., Yang, T., Gillett, D. L., Leis, A. P., Morton, C. J., Kuiper, M. J., Parker, M. W., Spillman, N. J., Wong, W., Tsu, C., Dick, L. R., Griffin, M., & Tilley, L. (2019). The structure of the PA28-20S proteasome complex from Plasmodium falciparum and implications for proteostasis. Nature microbiology, 4(11), 1990–2000. https://doi.org/10.1038/s41564-019-0524-4
28. Arellano-Garcia, M. E., Misuno, K., Tran, S. D., & Hu, S. (2014). Interferon-γ induces immunoproteasomes and the presentation of MHC I-associated peptides on human salivary gland cells. PloS one, 9(8), e102878. https://doi.org/10.1371/journal.pone.0102878
29. Cascio P. (2014). PA28αβ: the enigmatic magic ring of the proteasome?. Biomolecules, 4(2), 566–584. https://doi.org/10.3390/biom4020566
30. Zhang, Z., Clawson, A., Realini, C., Jensen, C. C., Knowlton, J. R., Hill, C. P., & Rechsteiner, M. (1998). Identification of an activation region in the proteasome activator REGalpha. Proceedings of the National Academy of Sciences of the United States of America, 95(6), 2807–2811. https://doi.org/10.1073/pnas.95.6.2807
31. Li, J., Gao, X., Joss, L., & Rechsteiner, M. (2000). The proteasome activator 11 S REG or PA28: chimeras implicate carboxyl-terminal sequences in oligomerization and proteasome binding but not in the activation of specific proteasome catalytic subunits. Journal of molecular biology, 299(3), 641–654. https://doi.org/10.1006/jmbi.2000.3800
32. Chen, J., Wang, Y., Xu, C., Chen, K., Zhao, Q., Wang, S., Yin, Y., Peng, C., Ding, Z., & Cong, Y. (2021). Cryo-EM of mammalian PA28αβ-iCP immunoproteasome reveals a distinct mechanism of proteasome activation by PA28αβ. Nature communications, 12(1), 739. https://doi.org/10.1038/s41467-021-21028-3
33. Song, X., Mott, J. D., von Kampen, J., Pramanik, B., Tanaka, K., Slaughter, C. A., & DeMartino, G. N. (1996). A model for the quaternary structure of the proteasome activator PA28. The Journal of biological chemistry, 271(42), 26410–26417. https://doi.org/10.1074/jbc.271.42.26410
34. Li, N., Lerea, K. M., & Etlinger, J. D. (1996). Phosphorylation of the proteasome activator PA28 is required for proteasome activation. Biochemical and biophysical research communications, 225(3), 855–860. https://doi.org/10.1006/bbrc.1996.1263
35. Li, J., & Rechsteiner, M. (2001). Molecular dissection of the 11S REG (PA28) proteasome activators. Biochimie, 83(3-4), 373–383. https://doi.org/10.1016/s0300-9084(01)01236-6
36. Bose, S., Stratford, F. L., Broadfoot, K. I., Mason, G. G., & Rivett, A. J. (2004). Phosphorylation of 20S proteasome alpha subunit C8 (alpha7) stabilizes the 26S proteasome and plays a role in the regulation of proteasome complexes by gamma-interferon. The Biochemical journal, 378(Pt 1), 177–184. https://doi.org/10.1042/BJ20031122
37. Masselink, L. (2020). Influences of the phosphorylation status of PA28 to the activation of the 20S proteasome. Unpublished master report Biomolecular Sciences, Vrije Universiteit Amsterdam
38. Adelöf, J., Wiseman, J., Zetterberg, M., & Hernebring, M. (2021). PA28α overexpressing female mice maintain exploratory behavior and capacity to prevent protein aggregation in hippocampus as they age. Aging cell, 20(4), e13336. https://doi.org/10.1111/acel.13336
39. Wang, Q., Pan, F., Li, S., Huang, R., Wang, X., Wang, S., Liao, X., Li, D., & Zhang, L. (2019). The prognostic value of the proteasome activator subunit gene family in skin cutaneous melanoma. Journal of Cancer, 10(10), 2205–2219. https://doi.org/10.7150/jca.30612
40. Sánchez-Martín, D., Martínez-Torrecuadrada, J., Teesalu, T., Sugahara, K. N., Alvarez-Cienfuegos, A., Ximénez-Embún, P., Fernández-Periáñez, R., Martín, M. T., Molina-Privado, I., Ruppen-Cañás, I., Blanco-Toribio, A., Cañamero, M., Cuesta, A. M., Compte, M., Kremer, L., Bellas, C., Alonso-Camino, V., Guijarro-Muñoz, I., Sanz, L., Ruoslahti, E., … Alvarez-Vallina, L. (2013). Proteasome activator complex PA28 identified as an accessible target in prostate cancer by in vivo selection of human antibodies. Proceedings of the National Academy of Sciences of the United States of America, 110(34), 13791–13796. https://doi.org/10.1073/pnas.1300013110
41. Feng, X., Jiang, Y., Xie, L., Jiang, L., Li, J., Sun, C., Xu, H., Wang, R., Zhou, M., Zhou, Y., Dan, H., Wang, Z., Ji, N., Deng, P., Liao, G., Geng, N., Wang, Y., Zhang, D., Lin, Y., Ye, L., … Chen, Q. (2016). Overexpression of proteasomal activator PA28α serves as a prognostic factor in oral squamous cell carcinoma. Journal of experimental & clinical cancer research : CR, 35, 35. https://doi.org/10.1186/s13046-016-0309-z
42. Gu, Y., Barwick, B. G., Shanmugam, M., Hofmeister, C. C., Kaufman, J., Nooka, A., Gupta, V., Dhodapkar, M., Boise, L. H., & Lonial, S. (2020). Downregulation of PA28α induces proteasome remodeling and results in resistance to proteasome inhibitors in multiple myeloma. Blood cancer journal, 10(12), 125. https://doi.org/10.1038/s41408-020-00393-0
43. Zhang, D., Lim, S. G., & Koay, E. S. (2007). Proteomic identification of down-regulation of oncoprotein DJ-1 and proteasome activator subunit 1 in hepatitis B virus-infected well-differentiated hepatocellular carcinoma. International journal of oncology, 31(3), 577–584.
44. Zhang, J., Wang, K., Zhang, J., Liu, S. S., Dai, L., & Zhang, J. Y. (2011). Using proteomic approach to identify tumor-associated proteins as biomarkers in human esophageal squamous cell carcinoma. Journal of proteome research, 10(6), 2863–2872. https://doi.org/10.1021/pr200141c
45. Longuespée, R., Boyon, C., Castellier, C., Jacquet, A., Desmons, A., Kerdraon, O., Vinatier, D., Fournier, I., Day, R., & Salzet, M. (2012). The C-terminal fragment of the immunoproteasome PA28S (Reg alpha) as an early diagnosis and tumor-relapse biomarker: evidence from mass spectrometry profiling. Histochemistry and cell biology, 138(1), 141–154. https://doi.org/10.1007/s00418-012-0953-0
46. Merenda, A., Andersson-Rolf, A., Mustata, R. C., Li, T., Kim, H., & Koo, B. K. (2017). A Protocol for Multiple Gene Knockout in Mouse Small Intestinal Organoids Using a CRISPR-concatemer. Journal of visualized experiments : JoVE, (125), 55916. https://doi.org/10.3791/55916

47. Ahn, J. Y., Tanahashi, N., Akiyama, K., Hisamatsu, H., Noda, C., Tanaka, K., Chung, C. H., Shibmara, N., Willy, P. J., & Mott, J. D. (1995). Primary structures of two homologous subunits of PA28, a gamma-interferon-inducible protein activator of the 20S proteasome. FEBS letters, 366(1), 37–42. https://doi.org/10.1016/0014-5793(95)00492-r
48. Zhou F. (2009). Molecular mechanisms of IFN-gamma to up-regulate MHC class I antigen processing and presentation. International reviews of immunology, 28(3-4), 239–260. https://doi.org/10.1080/08830180902978120
49. Bell, M. R., Engleka, M. J., Malik, A., & Strickler, J. E. (2013). To fuse or not to fuse: what is your purpose?. Protein science : a publication of the Protein Society, 22(11), 1466–1477. https://doi.org/10.1002/pro.2356
50. Roosild, T. P., Castronovo, S., & Choe, S. (2006). Structure of anti-FLAG M2 Fab domain and its use in the stabilization of engineered membrane proteins. Acta crystallographica. Section F, Structural biology and crystallization communications, 62(Pt 9), 835–839. https://doi.org/10.1107/S1744309106029125
51. Zarei, A., Razban, V., Hosseini, S. E., & Tabei, S. (2019). Creating cell and animal models of human disease by genome editing using CRISPR/Cas9. The journal of gene medicine, 21(4), e3082. https://doi.org/10.1002/jgm.3082
52. Liu, M., Rehman, S., Tang, X., Gu, K., Fan, Q., Chen, D., & Ma, W. (2019). Methodologies for Improving HDR Efficiency. Frontiers in genetics, 9, 691. https://doi.org/10.3389/fgene.2018.00691
53. Keller, A. A., Maeß, M. B., Schnoor, M., Scheiding, B., & Lorkowski, S. (2018). Transfecting Macrophages. Methods in molecular biology (Clifton, N.J.), 1784, 187–195. https://doi.org/10.1007/978-1-4939-7837-3_18
54. Weischenfeldt, J., & Porse, B. (2008). Bone Marrow-Derived Macrophages (BMM): Isolation and Applications. CSH protocols, 2008, pdb.prot5080. https://doi.org/10.1101/pdb.prot5080
55. Mashel, T. V., Tarakanchikova, Y. V., Muslimov, A. R., Zyuzin, M. V., Timin, A. S., Lepik, K. V., & Fehse, B. (2020). Overcoming the delivery problem for therapeutic genome editing: Current status and perspective of non-viral methods. Biomaterials, 258, 120282. https://doi.org/10.1016/j.biomaterials.2020.120282
56. Nguyen, Q. A., & Nicoll, R. A. (2018). The GABAA Receptor β Subunit Is Required for Inhibitory Transmission. Neuron, 98(4), 718–725.e3. https://doi.org/10.1016/j.neuron.2018.03.046
57. Suryanarayanan, A., Liang, J., Meyer, E. M., Lindemeyer, A. K., Chandra, D., Homanics, G. E., Sieghart, W., Olsen, R. W., & Spigelman, I. (2011). Subunit Compensation and Plasticity of Synaptic GABA(A) Receptors Induced by Ethanol in α4 Subunit Knockout Mice. Frontiers in neuroscience, 5, 110. https://doi.org/10.3389/fnins.2011.00110
58. Wang, X., Gerber, A., Chen, W. Y., & Roeder, R. G. (2020). Functions of paralogous RNA polymerase III subunits POLR3G and POLR3GL in mouse development. Proceedings of the National Academy of Sciences of the United States of America, 117(27), 15702–15711. https://doi.org/10.1073/pnas.1922821117
59. Chang, Y. P., Chen, C. L., Chen, S. O., Lin, Y. S., Tsai, C. C., Huang, W. C., Wang, C. Y., Hsieh, C. Y., Choi, P. C., & Lin, C. F. (2011). Autophagy facilitates an IFN-γ response and signal transduction. Microbes and infection, 13(11), 888–894. https://doi.org/10.1016/j.micinf.2011.05.008
60. Burke, J. D., & Young, H. A. (2019). IFN-γ: A cytokine at the right time, is in the right place. Seminars in immunology, 43, 101280. https://doi.org/10.1016/j.smim.2019.05.002
61. Mezouar, S., & Mege, J. L. (2020). Changing the paradigm of IFN-γ at the interface between innate and adaptive immunity: Macrophage-derived IFN-γ. Journal of leukocyte biology, 108(1), 419–426. https://doi.org/10.1002/JLB.4MIR0420-619RR
62. Tanaka, K., & Kasahara, M. (1998). The MHC class I ligand-generating system: roles of immunoproteasomes and the interferon-gamma-inducible proteasome activator PA28. Immunological reviews, 163, 161–176. https://doi.org/10.1111/j.1600-065x.1998.tb01195.x
63. Soza, A., Knuehl, C., Groettrup, M., Henklein, P., Tanaka, K., & Kloetzel, P. M. (1997). Expression and subcellular localization of mouse 20S proteasome activator complex PA28. FEBS letters, 413(1), 27–34. https://doi.org/10.1016/s0014-5793(97)00864-8
64. Lee, J. E., Kim, S. Y., & Shin, S. Y. (2015). Effect of Repeated Freezing and Thawing on Biomarker Stability in Plasma and Serum Samples. Osong public health and research perspectives, 6(6), 357–362. https://doi.org/10.1016/j.phrp.2015.11.005
65. Munder, M., Mallo, M., Eichmann, K., & Modolell, M. (1998). Murine macrophages secrete interferon gamma upon combined stimulation with interleukin (IL)-12 and IL-18: A novel pathway of autocrine macrophage activation. The Journal of experimental medicine, 187(12), 2103–2108. https://doi.org/10.1084/jem.187.12.2103
66. Lino, C. A., Harper, J. C., Carney, J. P., & Timlin, J. A. (2018). Delivering CRISPR: a review of the challenges and approaches. Drug delivery, 25(1), 1234–1257. https://doi.org/10.1080/10717544.2018.1474964
67. Kuehn, L., & Dahlmann, B. (1997). Structural and functional properties of proteasome activator PA28. Molecular biology reports, 24(1-2), 89–93. https://doi.org/10.1023/a:1006897801858
68. Uniyal, A. P., Mansotra, K., Yadav, S. K., & Kumar, V. (2019). An overview of designing and selection of sgRNAs for precise genome editing by the CRISPR-Cas9 system in plants. 3 Biotech, 9(6), 223. https://doi.org/10.1007/s13205-019-1760-2
69. Zhang, Z., Realini, C., Clawson, A., Endicott, S., & Rechsteiner, M. (1998). Proteasome activation by REG molecules lacking homolog-specific inserts. The Journal of biological chemistry, 273(16), 9501–9509. https://doi.org/10.1074/jbc.273.16.9501
70. Realini, C., Jensen, C. C., Zhang, Z., Johnston, S. C., Knowlton, J. R., Hill, C. P., & Rechsteiner, M. (1997). Characterization of recombinant REGalpha, REGbeta, and REGgamma proteasome activators. The Journal of biological chemistry, 272(41), 25483–25492. https://doi.org/10.1074/jbc.272.41.25483
71. Preckel, T., Fung-Leung, W. P., Cai, Z., Vitiello, A., Salter-Cid, L., Winqvist, O., Wolfe, T. G., Von Herrath, M., Angulo, A., Ghazal, P., Lee, J. D., Fourie, A. M., Wu, Y., Pang, J., Ngo, K., Peterson, P. A., Früh, K., & Yang, Y. (1999). Impaired immunoproteasome assembly and immune responses in PA28-/- mice. Science (New York, N.Y.), 286(5447), 2162–2165. https://doi.org/10.1126/science.286.5447.2162
72. Terpe K. (2003). Overview of tag protein fusions: from molecular and biochemical fundamentals to commercial systems. Applied microbiology and biotechnology, 60(5), 523–533. https://doi.org/10.1007/s00253-002-1158-6
73. Einhauer, A., & Jungbauer, A. (2001). The FLAG peptide, a versatile fusion tag for the purification of recombinant proteins. Journal of biochemical and biophysical methods, 49(1-3), 455–465. https://doi.org/10.1016/s0165-022x(01)00213-5
74. Zaiss, D. M., & Kloetzel, P. M. (1999). A second gene encoding the mouse proteasome activator PA28beta subunit is part of a LINE1 element and is driven by a LINE1 promoter. Journal of

molecular biology, 287(5), 829–835. https://doi.org/10.1006/jmbi.1999.2656

75. Pickering, A. M., Koop, A. L., Teoh, C. Y., Ermak, G., Grune, T., & Davies, K. J. (2010). The immunoproteasome, the 20S proteasome and the PA28αβ proteasome regulator are oxidative-stress-adaptive proteolytic complexes. The Biochemical journal, 432(3), 585–594. https://doi.org/10.1042/BJ20100878
76. Pizzino, G., Irrera, N., Cucinotta, M., Pallio, G., Mannino, F., Arcoraci, V., Squadrito, F., Altavilla, D., & Bitto, A. (2017). Oxidative Stress: Harms and Benefits for Human Health. Oxidative medicine and cellular longevity, 2017, 8416763. https://doi.org/10.1155/2017/8416763
77. Yamano, T., Mizukami, S., Murata, S., Chiba, T., Tanaka, K., & Udono, H. (2008). Hsp90-mediated assembly of the 26 S proteasome is involved in major histocompatibility complex class I antigen processing. The Journal of biological chemistry, 283(42), 28060–28065. https://doi.org/10.1074/jbc.M803077200
78. Gough, D. J., Levy, D. E., Johnstone, R. W., & Clarke, C. J. (2008). IFNgamma signaling-does it mean JAK-STAT?. Cytokine & growth factor reviews, 19(5-6), 383–394. https://doi.org/10.1016/j.cytogfr.2008.08.004
79. Bose, S., Brooks, P., Mason, G. G., & Rivett, A. J. (2001). gamma-Interferon decreases the level of 26 S proteasomes and changes the pattern of phosphorylation. The Biochemical journal, 353(Pt 2), 291–297. https://doi.org/10.1042/0264-6021:3530291
80. Kors, S., Geijtenbeek, K., Reits, E., & Schipper-Krom, S. (2019). Regulation of Proteasome Activity by (Post-)transcriptional Mechanisms. Frontiers in molecular biosciences, 6, 48. https://doi.org/10.3389/fmolb.2019.00048
81. Pickering, A. M., Linder, R. A., Zhang, H., Forman, H. J., & Davies, K. (2012). Nrf2-dependent induction of proteasome and Pa28αβ regulator are required for adaptation to oxidative stress. The Journal of biological chemistry, 287(13), 10021–10031. https://doi.org/10.1074/jbc.M111.277145
82. Ossendorp, F., Fu, N., Camps, M., Granucci, F., Gobin, S. J., van den Elsen, P. J., Schuurhuis, D., Adema, G. J., Lipford, G. B., Chiba, T., Sijts, A., Kloetzel, P. M., Ricciardi-Castagnoli, P., & Melief, C. J. (2005). Differential expression regulation of the alpha and beta subunits of the PA28 proteasome activator in mature dendritic cells. Journal of immunology (Baltimore, Md. : 1950), 174(12), 7815–7822. https://doi.org/10.4049/jimmunol.174.12.7815
83. Otoda, T., Takamura, T., Misu, H., Ota, T., Murata, S., Hayashi, H., Takayama, H., Kikuchi, A., Kanamori, T., Shima, K. R., Lan, F., Takeda, T., Kurita, S., Ishikura, K., Kita, Y., Iwayama, K., Kato, K., Uno, M., Takeshita, Y., Yamamoto, M., … Kaneko, S. (2013). Proteasome dysfunction mediates obesity-induced endoplasmic reticulum stress and insulin resistance in the liver. Diabetes, 62(3), 811–824. https://doi.org/10.2337/db11-1652
84. Yadranji Aghdam, S., & Mahmoudpour, A. (2016). Proteasome Activators, PA28α and PA28β, Govern Development of Microvascular Injury in Diabetic Nephropathy and Retinopathy. International journal of nephrology, 2016, 3846573. https://doi.org/10.1155/2016/3846573
85. Tsihlis, N. D., Rodriguez, M. P., Jiang, Q., Schwartz, A., Flynn, M. E., Vercammen, J. M., & Kibbe, M. R. (2016). Nitric oxide differentially affects proteasome activator 28 after arterial injury in type 1 and type 2 diabetic rats. The Journal of surgical research, 202(2), 413–421. https://doi.org/10.1016/j.jss.2016.01.030
86. Uttara, B., Singh, A. V., Zamboni, P., & Mahajan, R. T. (2009). Oxidative stress and neurodegenerative diseases: a review of upstream and downstream antioxidant therapeutic options. Current neuropharmacology, 7(1), 65–74. https://doi.org/10.2174/157015909787602823
87. Zaiss, D. M., Standera, S., Holzhütter, H., Kloetzel, P., & Sijts, A. J. (1999). The proteasome inhibitor PI31 competes with PA28 for binding to 20S proteasomes. FEBS letters, 457(3), 333–338. https://doi.org/10.1016/s0014-5793(99)01072-8
88. Seeger, M., Ferrell, K., Frank, R., & Dubiel, W. (1997). HIV-1 tat inhibits the 20 S proteasome and its 11 S regulator-mediated activation. The Journal of biological chemistry, 272(13), 8145–8148. https://doi.org/10.1074/jbc.272.13.8145
89. Stohwasser, R., Holzhütter, H. G., Lehmann, U., Henklein, P., & Kloetzel, P. M. (2003). Hepatitis B virus HBx peptide 116-138 and proteasome activator PA28 compete for binding to the proteasome alpha4/MC6 subunit. Biological chemistry, 384(1), 39–49. https://doi.org/10.1515/BC.2003.005
90. Li, J., Powell, S. R., & Wang, X. (2011). Enhancement of proteasome function by PA28α overexpression protects against oxidative stress. FASEB journal: official publication of the Federation of American Societies for Experimental Biology, 25(3), 883–893. https://doi.org/10.1096/fj.10-160895
91. Li, S., Dai, X., Gong, K., Song, K., Tai, F., & Shi, J. (2019). PA28α/β Promote Breast Cancer Cell Invasion and Metastasis via Down-Regulation of CDK15. Frontiers in oncology, 9, 1283. https://doi.org/10.3389/fonc.2019.01283
92. Pickering, A. M., & Davies, K. J. (2012). Degradation of damaged proteins: the main function of the 20S proteasome. Progress in molecular biology and translational science, 109, 227–248. https://doi.org/10.1016/B978-0-12-397863-9.00006-7
93. Pickering, A. M., & Davies, K. J. (2012). Degradation of damaged proteins: the main function of the 20S proteasome. Progress in molecular biology and translational science, 109, 227–248. https://doi.org/10.1016/B978-0-12-397863-9.00006-7

7. Supplementary data.

7.1 Tables.

Table S1: Potential sgRNAs selected from Benchling using the *Psme1* gene as input query. Potential sgRNA targeting 249Y. Copied from Benchling. *Abbreviations: PAM, protospacer adjacent motif.*

Cutting position	Sequence of the sgRNAs	PAM type	On-target score	Off-target score
56200199	GAAGCCCCGTGGAGAAACCA	AGG	30.1	28.1
56200200	AAGCCCCGTGGAGAAACCAA	GGG	36.4	28.2
56200205	GGCTCAATAGATCATTCCCT	TGG	36.8	30.2
56200226	CCATCACAGAATGAGAGAGG	GGG	69.3	27.6
56200227	CCCATCACAGAATGAGAGAG	GGG	66.8	26.5
56200228	ACCCATCACAGAATGAGAGA	GGG	55.0	24.5
56200229	TACCCATCACAGAATGAGAG	AGG	63.6	26.4

Table S2: Potential sgRNAs selected from Benchling using the *Psme1* gene as input query. Potential sgRNA targeting 239k. Copied from Benchling. *Abbreviations: PAM, protospacer adjacent motif.*

Cutting position	Sequence of the sgRNAs	PAM type	On-target score	Off-target score
56200199	GAAGCCCCGTGGAGAAACCA	AGG	30.1	28.1
56200200	AAGCCCCGTGGAGAAACCAA	GGG	36.4	28.2

Table S3: full sequence of primers ordered which are in turn annealed to create gRNAs.

Targeting	Cassette	Sequence of sgRNA primers including overhangs
249Y	1	FWD: CACCGGCTCTCTCATTCTGTGATGGGGT REV: TAAAACCCCATCACAGAATGAGAGAGCC
249Y	2	FWD: ACCGGCTCTCTCATTCTGTGATGGGG REV: AAAACCCCATCACAGAATGAGAGAGC
239K	1	FWD: CACCGGGAGAAGCTCAAGAAGCCCCGGT REV: TAAAACCGGGGCTTCTTGAGCTTCTCCC
239K	2	FWD: ACCGGGAGAAGCTCAAGAAGCCCCGG REV: AAAACCGGGGCTTCTTGAGCTTCTCC

Table S4: full sequence of the designed HDR templates used in this study. In bold the modified sequence compared to the target DNA is visualized. *Abbreviations: Y, tyrosine; E, glutamic acid; P, phenylalanine; K, lysine; HDR, homology directed repair; Ref, reference.*

Targeting	Modification	HDR template sequence	Ref.
N-terminus *Psme1*	Inserting FLAG-tag	TCCCCAAACCCAGGAAGGCCGTGCAGGTTTCGAGCTGTGCTTTCGCTTTCCCTTCCCGCTGCCCACCCCA GGTTCCTCGTGCGGCGCTCACCACCACCCCCCGGCTCTGGCCATG**GATTACAAAGACGATGACGACAAG** GCCACACTGAGGGTCCATCCCGAAGCCCAAGCCAAGGTGAGCGTTGCGGGTTCGAGTGGGGAGTAGA GGCTTTAGAGAGGCGTGGTTCAGAGCAGACCAGAGCTCTGGGGGAGCCCACTT	[37]
249Y	Y -> E	GGGCCCGTGGCTGACCTCCACCACTCTGTGCTCCGATAGGCTGTGTTATATGACATCATCCTGAAGAACT TTGAGAAGCTCAAGAAGCCCCGTGGAGAAACCAAGGGAATGATC**GAG**TGAGCACCCTCTCTCATTCTGT GATGGGTATAGCAGAAACCTTCCTGCTTTTCACCAGGAACTCTAGACTGGACGCAGTCTTCTTCCTACTG GCTGGGGTTTCTCCCTCACTCTGCCTCCC	
249Y	Y -> P	GGCCCGTGGCTGACCTCCACCACTCTGTGCTCCGATAGGCTGTGTTATATGACATCATCCTGAAGAACTTT GAGAAGCTCAAGAAGCCCCGTGGAGAAACCAAGGGAATGATC**TTT**TGAGCACCCTCTCTCATTCTGTGAT GGGTATAGCAGAAACCTTCCTGCTTTTCACCAGGAACTCTAGACTGGACGCAGTCTTCTTCCTACTGGCTG GGGTTTCTCCCTCACTCTGCCTCC	
239K	K -> STOP	/	

Table S5: Values of the quantification of the western blot. *Values correspond to ImageJ analysis, representative histograms and boxing strategy are shown in* ***figure S2****.*

Subunit	Measured	Raw values ImageJ	Background subtracted
PA28β	Background	519.021	
	Unstimulated sample 1	14.992.421	14.473.400
	Unstimulated sample 2	15.219.664	14.700.643
	Unstimulated sample 3	10.629.430	10.110.409
	Stimulated sample 1	13.406.765	12.887.744
	Stimulated sample 2	12.836.865	12.317.844
	Stimulated sample 3	12.975.865	12.456.844
PA28α	Background	1.430.991	
	Unstimulated sample 1	24.709.090	23.278.099
	Unstimulated sample 2	24.633.676	23.202.685
	Unstimulated sample 3	25.909.262	24.478.271
	Stimulated sample 1	26.347.848	24.916.857
	Stimulated sample 2	27.074.848	25.643.857
	Stimulated sample 3	26.550.848	25.119.857

7.1 Figures.

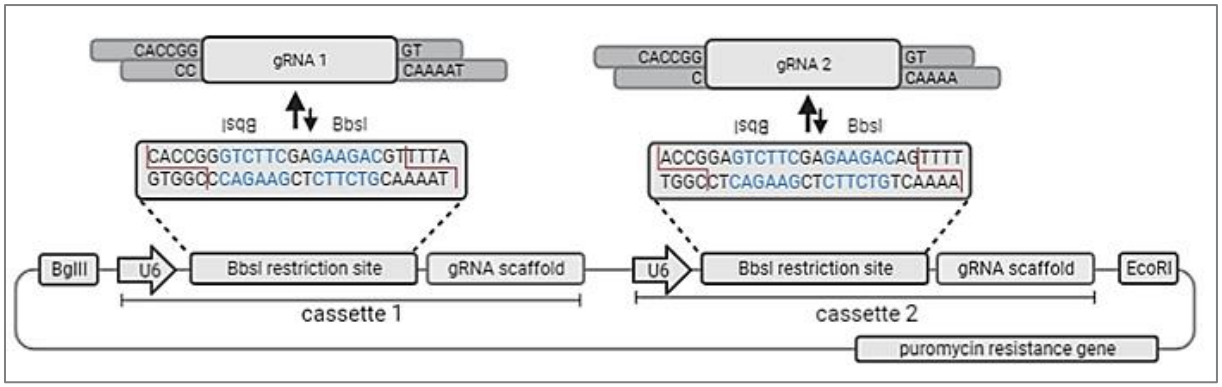

Figure S1: Design of the concatemer used to create the different cell lines*.* Schematic representation of the used CRISPR-concatemer for creating a double knock-out, adapted from Merenda et al. (2017)[46]. The scheme shows a CRISPR-concatemer with 2 cassettes, containing a U6 promotor, two BbsI restriction sites and a gRNA scaffold (i.e., Cas9 binding site) respectively. During the shuffling reaction, the BbsI restriction sites are replaced with the provided gRNA fragments which contain matching overhangs, resulting in losing the restriction sites, preventing recutting. In blue: BbsI recognition sites. Red annotations: cutting site BbsI enzyme *Abbreviations: gRNA, guide RNA.*

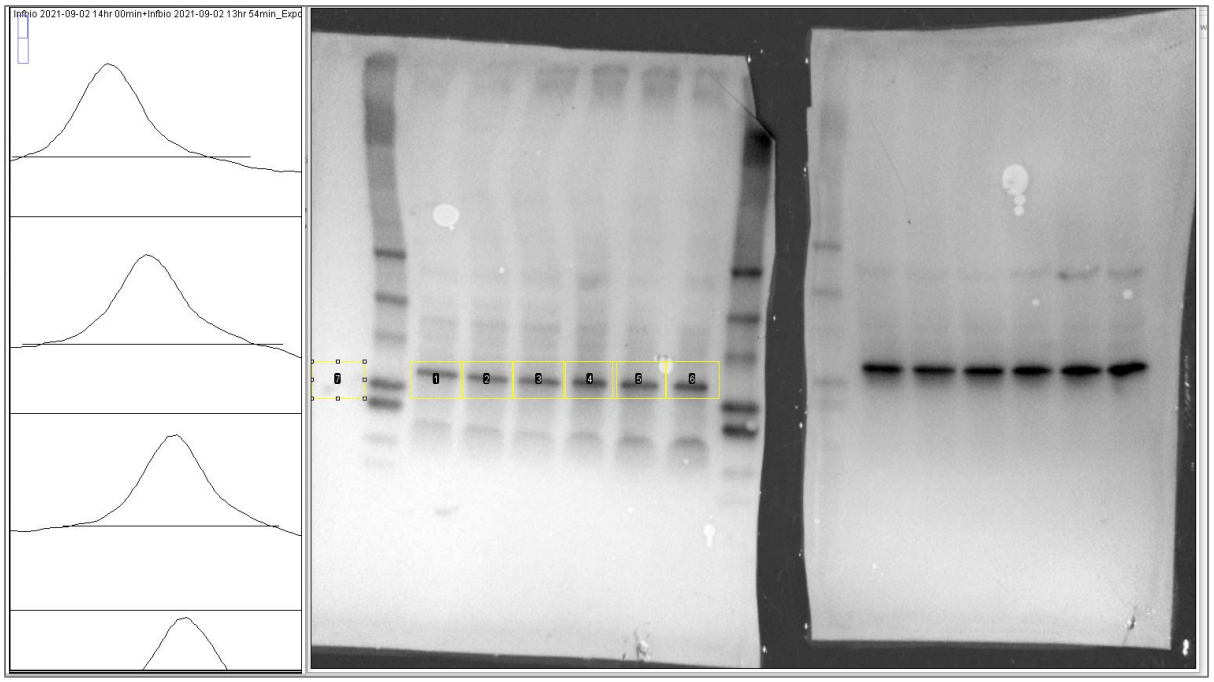

Figure S2: representative plot of quantitative western blot analysis using ImageJ. *The western blot of* ***figure S3*** *was quantified using ImageJ. First, the rectangular selections tool from the ImageJ was used to place a box around the first band to analyse. This same rectangle (in terms of height and area covered) was also put around the other bands to analyse as well as on an empty lane to be able to remove background noise from the values later on. Due to the lack of an empty lane, the background-rectangle was placed at the left side of the left marker. Using the straight-line selection tool from the ImageJ toolbar, a line was drawn on the bottom of the corresponding histograms to make it close completely (left panel). Next, the wand tool was used to highlight on the areas closed in the previous steps (values can be found in* ***table S5****). The background value was subtracted from the other values, and these corrected values were statistically analyzed and visualised using GraphPad Prism 9 (nonparametric Mann Whitney test). The histograms on the left side correspond (from top to bottom) with the rectangular boxes 1, 2 and 3, respectively.*

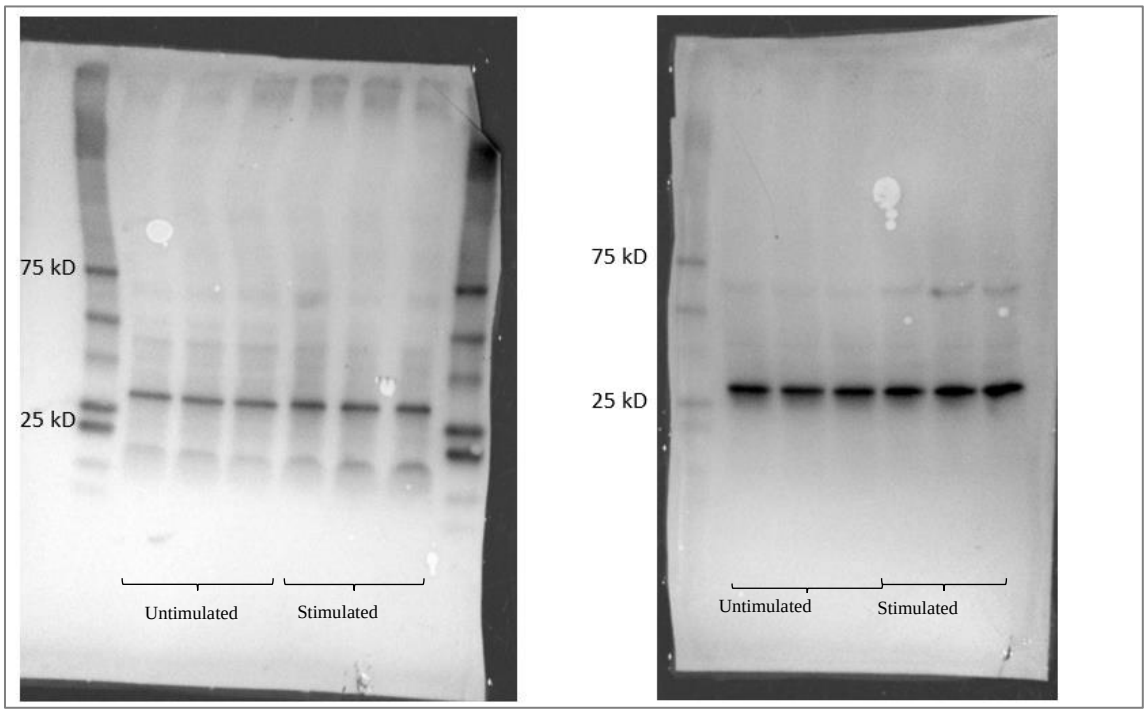

Figure S3: full western blot figure of the PA28αβ quantification. *Ana-1 cells were cultured overnight with or without 50 ng/µl IFN-γ. Subsequently, the total lysate of these cells was run on a western blot and probed with either anti-PA28α (left blot) or anti-PA28β antibodies (right blot). Used ladder: precision plus marker.*

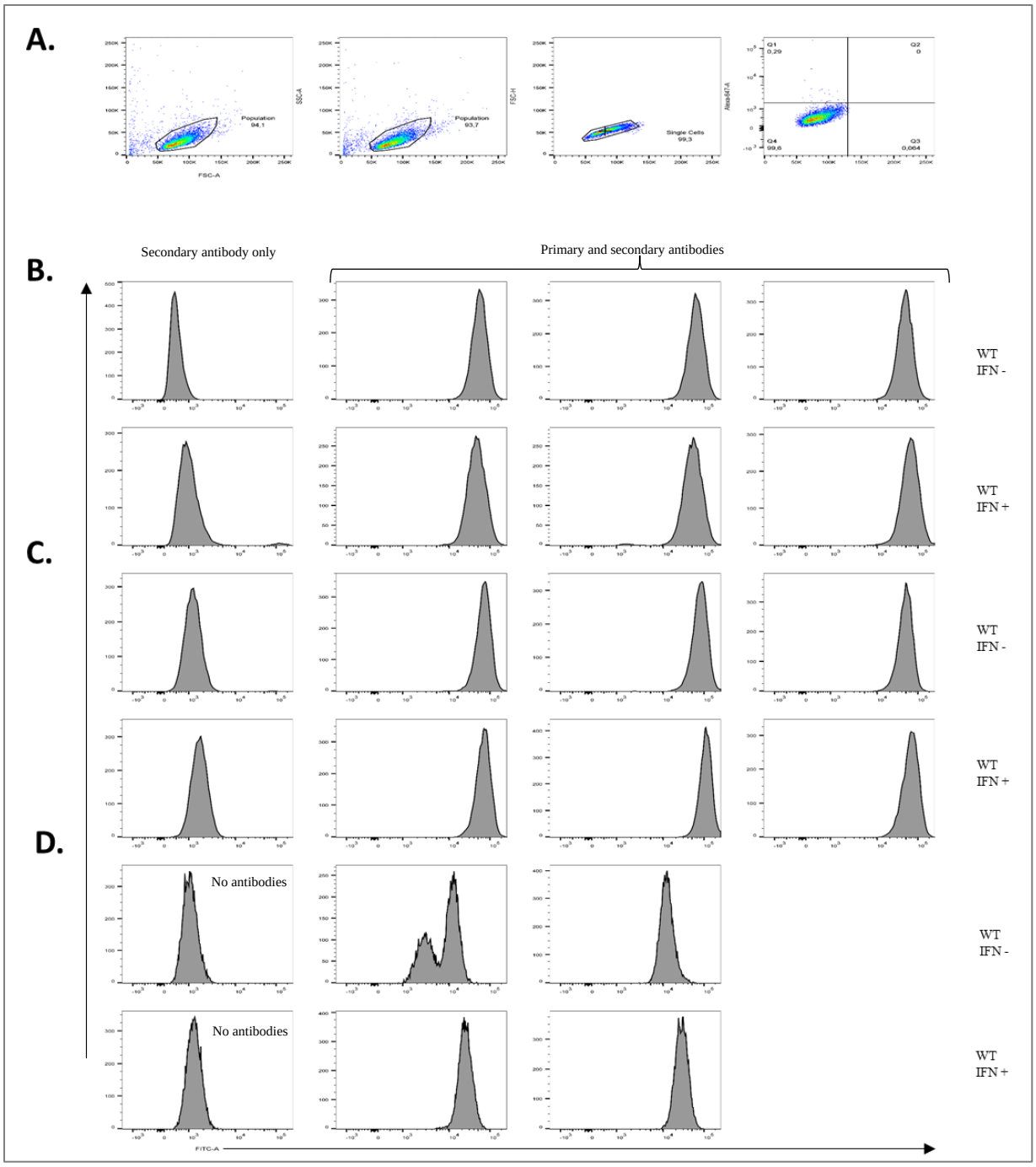

Figure S4: corresponding histograms of the expression levels of intracellular PA28α, PA28ß and extracellular MHC class I complexes in Ana-1 cells from figure 4. (A) *gating strategy of the analysis procedure. First, gating the living cells from the debris in the FSC-A vs SSC-A plot. Second, in the FSC-H vs FSC-A plot selecting the single cells. Lastly, determining the base level for PA28αß by setting the base-level expression using a sample only stained with secondary antibody. This step was done for both unstimulated and stimulated cells. Same procedure was used for MHC class I base level expression. For* ***(B) and (C)*** *on top is visualized which antibodies were used for the column, and on the right side of the histograms is noted if interferon was added or not.* ***(B)*** *These samples were stained against PA28α,* ***(C)*** *was stained against PA28ß and* ***(D)*** *was stained against MHC class I (subtype H2Kb). Moreover, the first column of D entails wildtype cells without any antibody, due to the fact the primary and secondary antibody are conjugated together.*

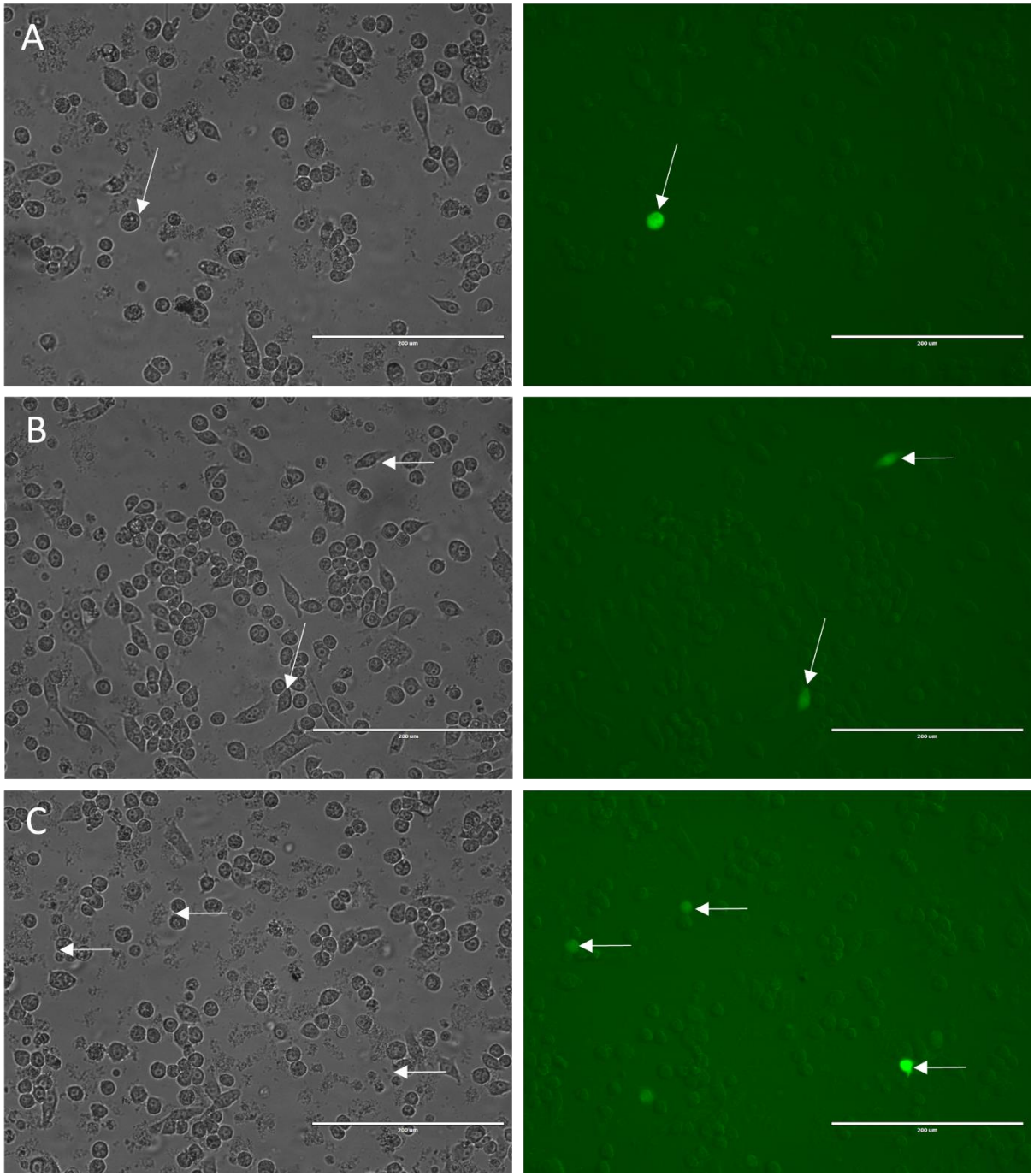

Figure S5: eGFP expression in Ana-1 cells after electroporation with an eGFP encoding plasmid ~28h prior. *Around 1 almost full-grown dish of Ana-1 cells was electroporated with either* ***a.*** *3 µl,* ***b.*** *6 µl or* ***c.*** *9 µl of eGFP encoding plasmid. eGFP expression was visualized using a light microscope after ~28h.*

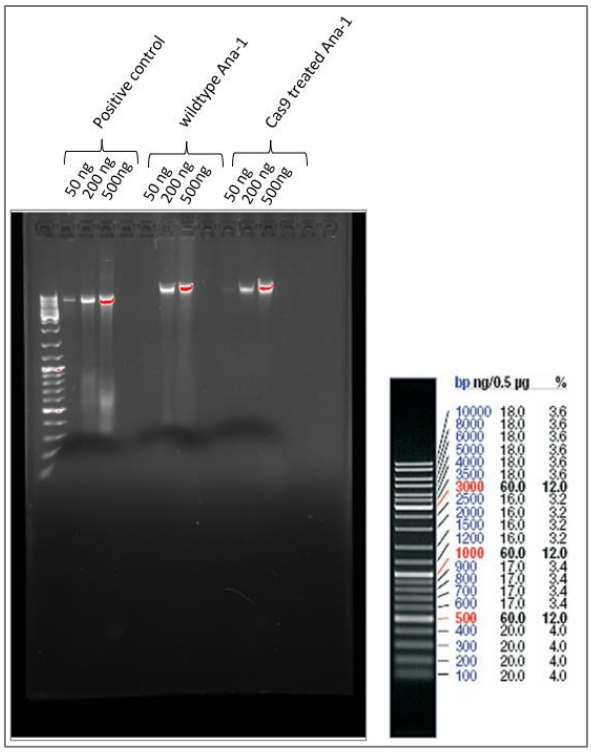

Figure S6: full figure of confirmation of successful genomic extraction. *Genomic extraction was performed using a genomic extraction kit and the provided instructions. Subsequently, a digestion reaction was performed using the NRU1 enzyme and either 50, 200 or 500 ng genomic DNA as starting concentration. Ladder (right panel) used: gene ruler mix (retrieved from manufacturer's instructions (ThermoFisher; USA).*

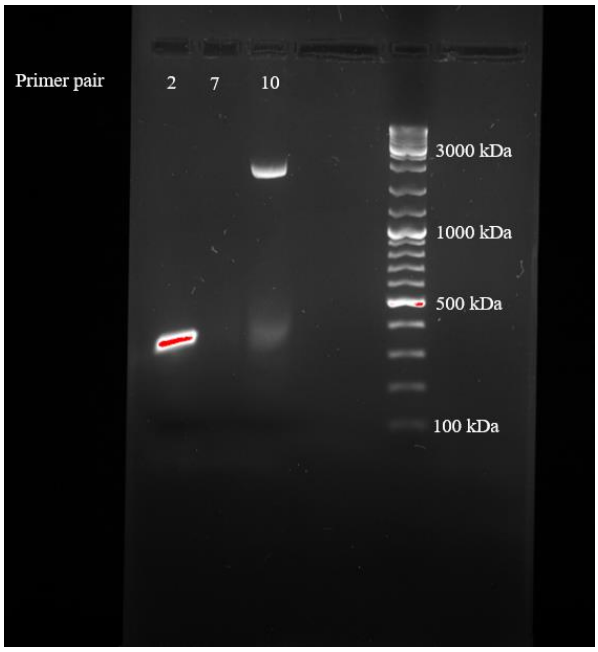

Figure S7: full figure primer pair optimisation. *A PCR reaction as run using the Q5 enzyme and 200 ng genomic DNA. Thereafter, 15 µL of the PCR product was loaded onto a 1% agar gel. Ladder used: gene ruler mix.*

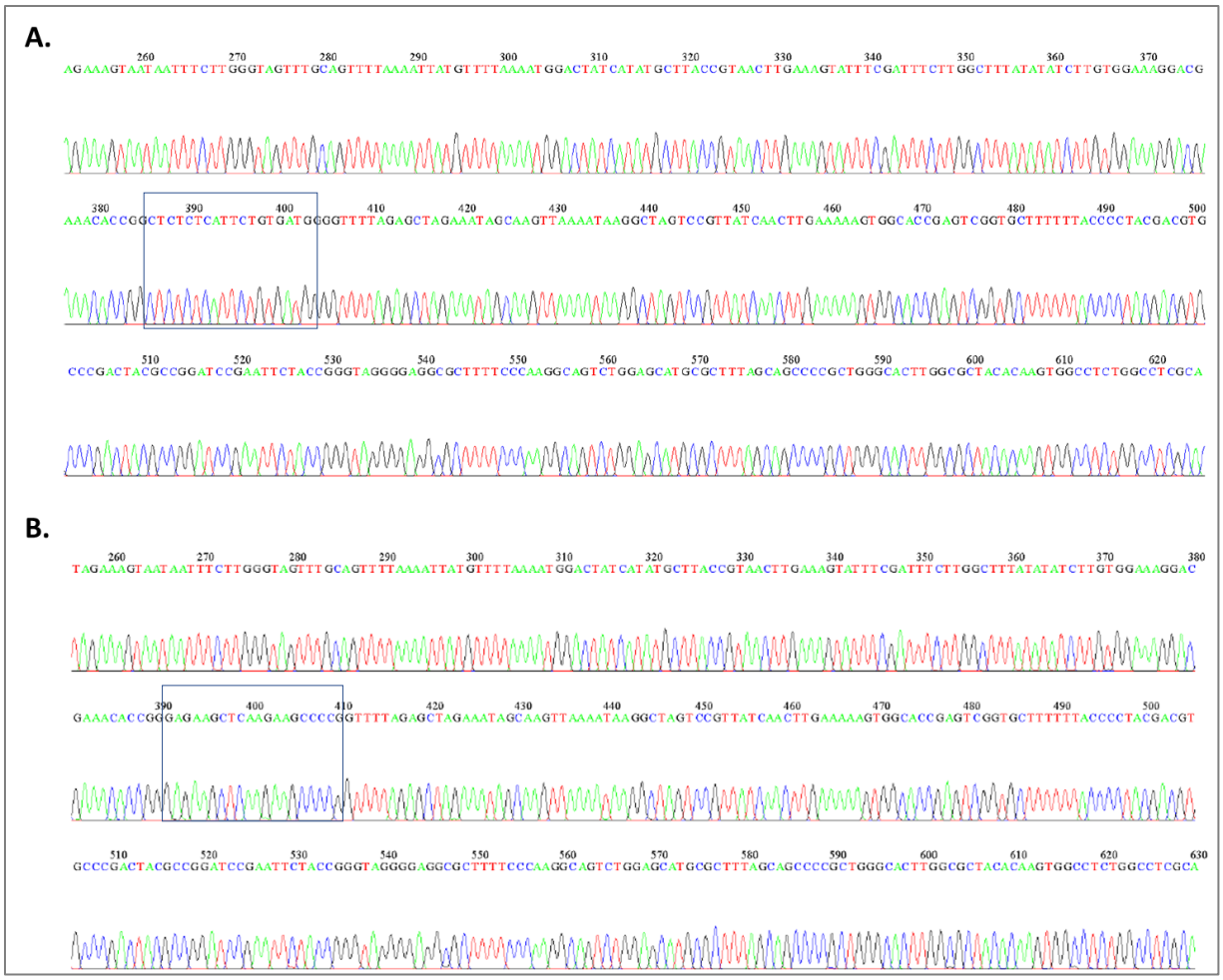

Figure S8: sanger sequencing of filled cassettes. *Both (**A**) and (**B**) entail a screenshot of a part of the sanger sequencing results in which the filled cassette is boxed (both cassette 1), whereas the empty second cassette is not shown. **(A)** shows the filled cassette which targets 249Y of Psme1. (**B**) shows the cassette filled targeting 239K (disordered segment removal). Sanger sequencing was performed by Macrogen (Netherlands) and analyzed using Chromas.*

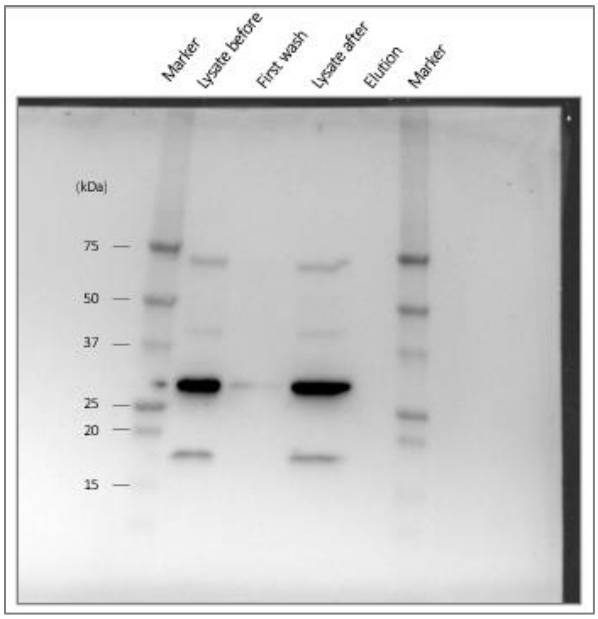

Figure S9: full western blot figure of immunoprecipitation of PA28β. *The lanes were loaded with (from left to right) the precision pls marker, lysate before the beads were added, fluid used to wash the beads after incubation with the lysate, lysate after the incubation overnight with the beads, elution fraction and again a precision plus marker. After loading, the lanes were electrophoresed on a SDS-PAGE gel and transferred to a polyvinylidene difluoride membrane. Primary antibody used for protein detection are specific for rabbit PA28β, and secondary is specific for rabbit-antibodies. Ladder used: precision plus.*

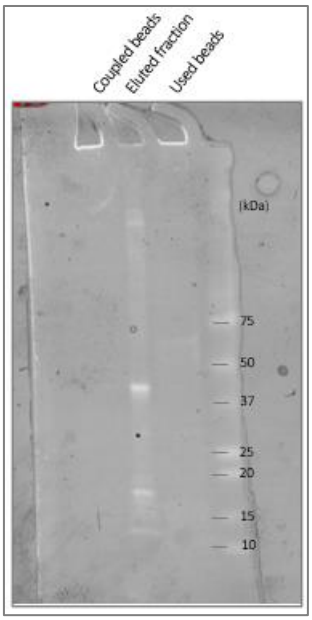

Figure S10: full figure of the Coomassie staining of the coupled beads, eluted fraction, and the used beads. *The lanes were loaded with (from left to right) beads coupled to the antibody targeting PA28β, the eluted fraction also used in the western blot from **figure S9**, and the beads used to capture PA28β from the lysate. After loading, it was electrophoresed on a SDS-PAGE gel and stained with Coomassie Blue for ~1h. Ladder used: precision plus.*